

Lehigh University Lehigh Preserve

Fritz Laboratory Reports

Civil and Environmental Engineering

1983

Laboratory study of ground response to dynamic densification march 15, 1983

Hsai-Yang Fang

Glenn W. Ellis

Follow this and additional works at: <http://preserve.lehigh.edu/engr-civil-environmental-fritz-lab-reports>

Recommended Citation

Fang, Hsai-Yang and Ellis, Glenn W., "Laboratory study of ground response to dynamic densification march 15, 1983" (1983). *Fritz Laboratory Reports*. Paper 2245.
<http://preserve.lehigh.edu/engr-civil-environmental-fritz-lab-reports/2245>

This Technical Report is brought to you for free and open access by the Civil and Environmental Engineering at Lehigh Preserve. It has been accepted for inclusion in Fritz Laboratory Reports by an authorized administrator of Lehigh Preserve. For more information, please contact preserve@lehigh.edu.

PROGRESS REPORT

LABORATORY STUDY OF GROUND RESPONSE TO DYNAMIC DENSIFICATION

H. Y. Fang and G. W. Ellis

This work was conducted under the sponsorship of Construction Materials Technology, Inc., International. The opinions, findings, and conclusions expressed in this report are those of the authors, and are not necessarily those of the project sponsor.

Fritz Engineering Laboratory
Department of Civil Engineering
Lehigh University
Bethlehem, Pennsylvania

March 15, 1983

Fritz Engineering Laboratory Report No. 462.6

PROGRESS REPORT

LABORATORY STUDY OF GROUND RESPONSE TO DYNAMIC DENSIFICATION

by

H. Y. Fang¹ and G. W. Ellis²

KEY WORDS: Soil Mechanics, Foundation, Testing, Materials, Modeling, Instrumentation, Dynamics, Compaction, Densification, Consolidation.

ABSTRACT:

This progress report presents the laboratory test results of dynamic densification (consolidation) on three distinct types of fill material including clay, sand and flyash (silt). Various weights or poulder sizes, thickness of fill deposits, and densification energy relating to the measured ground response are measured and evaluated. The ground response is measured by use of the pressure cell and the loads applied to the ground are controlled by an electromagnetic system. All results are summarized in graphical form including the effect of the poulder size, densification energy, soil type and number of drops of the poulder.

-
1. Professor and Director, Geotechnical Engineering Division, Lehigh University, Bethlehem, PA 18015.
 2. Research Assistant, Geotechnical Engineering Division, Lehigh University, Bethlehem, PA 18015.

Table of Contents

Key Words	i
Abstract	i
1. Introduction	1
2. Soil-Pounder Interaction	5
3. Laboratory Experimental Study	8
3.1 Material	8
3.2 Test Equipment and Instrumentation	8
3.3 Test Procedure	12
4. Summary of Test Results and Discussion	23
4.1 Thickness of Fill and Pounder Area	23
4.2 Ground Response and Densification Energy	27
4.3 Crater Profile	28
4.4 Crater Area and Volume	35
4.5 Number of Drops	35
5. Summary and Conclusions	41
Acknowledgement	42
References	44

LABORATORY STUDY OF GROUND RESPONSE TO DYNAMIC DENSIFICATION

1. INTRODUCTION

Dynamic densification is a mechanical process to consolidate loose soil deposits at great depths. The process used at the present time is not new. The largest construction project using this technique was during World War II in early 1940 when an airfield was built in Kunming, southwest China for Flying Tiger B-29 bomber landings. The method is frequently used around the world, especially in China, yet the little publicity given to it has encouraged little scientific study of the process. Figure 1 shows an early model of the dynamic densification equipment used in 1957 in China. The total pounder weight is about 36 to 72 kN dropped from 10m. In 1970, Menard Group (Menard and Broise, 1975) gave a scientific approach for the analysis of the dynamic densification process in which they included vibration during the in-situ consolidation process in correlation with basic geotechnical parameters and field subsurface investigations. Since then, this method has been widely used in many large-scale construction projects for densification of deep granular soils in Sweden, England, Australia, Germany, France as well as in the U.S.A. It also shows some success on soft clays (Qian, et al., 1980; Ramaswamy, et al., 1981). The dynamic densification equipment currently used in construction is shown in Fig. 2. The total pounder weight has reached as much as 200 tons (1,779 kN) and the height of drop has reached as high as 40m.

The term 'dynamic densification' is known by several different names. The trade name used in the construction field in China is called 'Flying-Goose'. DeBeer and Vambeke (1973), West and Slocombe (1973), ASCE (1978) and Menard

Group use the name 'dynamic consolidation'. Leonards, Cutter and Holtz (1980a, 1980b) utilize the term 'dynamic compaction'. Lukeas (1980) describes the process as 'densification by pounding'. The Hayward Baker Company has a registered trademark for the technique called 'dynamic deep compaction'. The term 'ground modification' is also a registered trademark of the Hayward Baker Company (1981).

In strict accordance with generally accepted soil mechanics terminology, the densification of partially saturated deposits at constant moisture content, whether they be granular or cohesive, is termed 'compaction'. Alternately, densification of saturated deposits with decreasing water content, whether they be cohesive or granular, is termed 'consolidation'. Hence, the term dynamic compaction is applicable to densification of deposits above the water table at constant water content, whereas dynamic consolidation is applicable to saturated deposits at decreasing water content. The term 'dynamic densification' is utilized throughout this report to denote either dynamic consolidation or dynamic compaction.

Because the art of the in-situ dynamic densification process has kept ahead of the analytical process, numerous technical questions exist, such as the effective size of the poulder, the effective depth, material types, rate of porewater dissipation, percent of energy transfer from poulder into ground soil, and soil-poulder interaction during the densification process. The purpose of this report is an attempt to answer some of these questions including (1) the effect of the poulder size and weight, (2) effects on various soil types; including clay, sand and silt (flyash); and (3) the effect of the number of drops of the poulder.

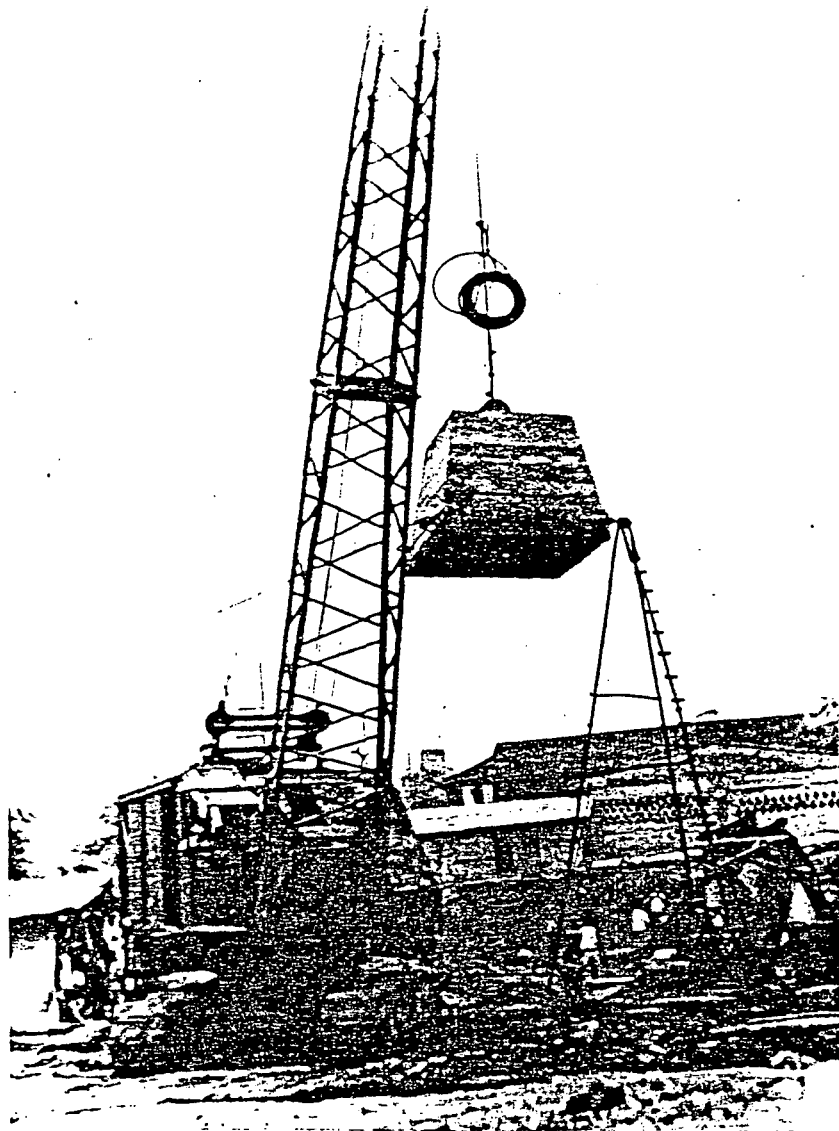


Figure 1 'Flying-Goose' Chinese Type Dynamic Compaction Equipment Built in 1957 Used for Roadways and Airfield Construction.
(Courtesy of Szechwan Provincial Construction Research Institute).

Site: Botlek
Client: Pan Ocean
Consultant/Contractor: Moss

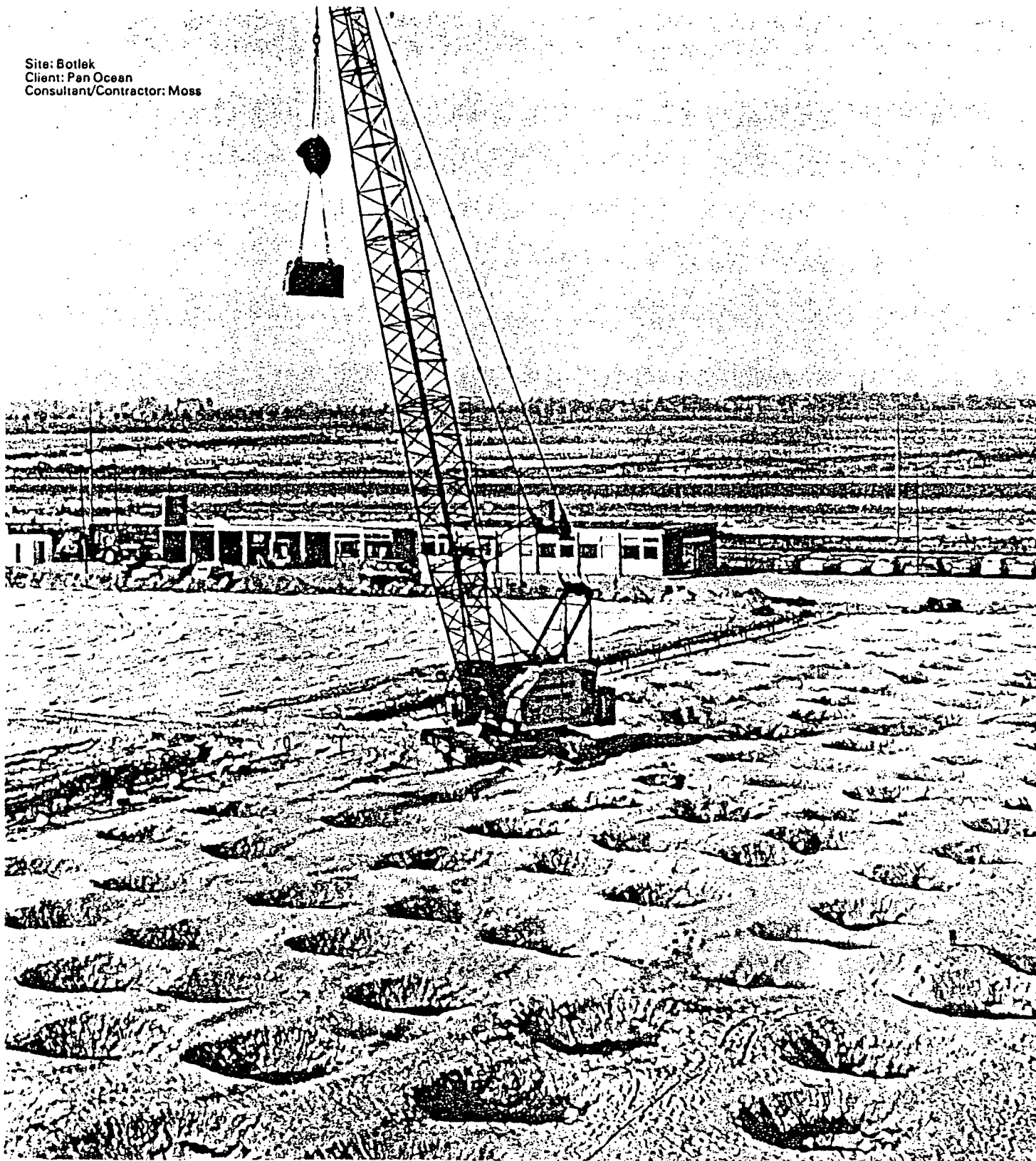


Figure 2 Dynamic Densification Equipment Currently Used
in Modern Construction
(Courtesy of Menard Group)

2. SOIL-POUNDER INTERACTION

When the pounder (weight) is applied to the soil mass (see Figs. 2 and 3), deformation may result from:

- (1) Immediate elastic and inelastic deformation of the soil structure.
 - (2) Pore water drained from the soil mass.
 - (3) Continuous time dependent or viscous flow under shear stress resulting in reorientation of the soil particles, and
 - (4) A combination of all the above which in most cases occurs simultaneously.
- However, it will depend upon soil properties, drainage conditions, stress history and environmental conditions.

Currently, the deep dynamic densification process is used mainly for granular soil at great depths. However, its use has been extended to the cohesive clays or silts. For practical applications the following parameters, which are directly related to the performance of the densification process, are important:

Material Type:

From the strength of material theory, the elastic properties of bodies are indicated by the coefficient of restitution, i.e., for the idealized elastic body this coefficient is 1.0, and for the inelastic body it is zero. For the in-situ soil, the coefficient lies between these two extremes varying with soil type and moisture content. The coefficient of restitution of a silt and clay are different from that of a granular soil.

Energy Losses:

The energy used by the poulder to temporarily compress an elastic body is given by the area under the load-strain curve. For idealized bodies this curve is assumed to be a straight line.

Effective Depth:

The effective depth or depth of influence is defined as how deep the poulder (weight), dropped freely from a certain height, will affect the fill material below the ground surface. Menard and Broise (1975) proposed that the effective depth is equal to:

$$D_e = \sqrt{Wh_x} \quad (1)$$

Later Leonards, Cutter and Holtz (1980) modified as:

$$D_e = 0.5 \sqrt{Wh_x} \quad (2)$$

where D_e = Effective depth

W = Weight of poulder

h_x = Height of Free Drop

The above Eqs (1) and (2) have been frequently used by practicing engineers for field control. The equations do not consider the type of fill materials, depth and size of the poulder. Therefore, some additional parameters are considered for evaluation of the effective depth through the laboratory investigation as described in the following sections.

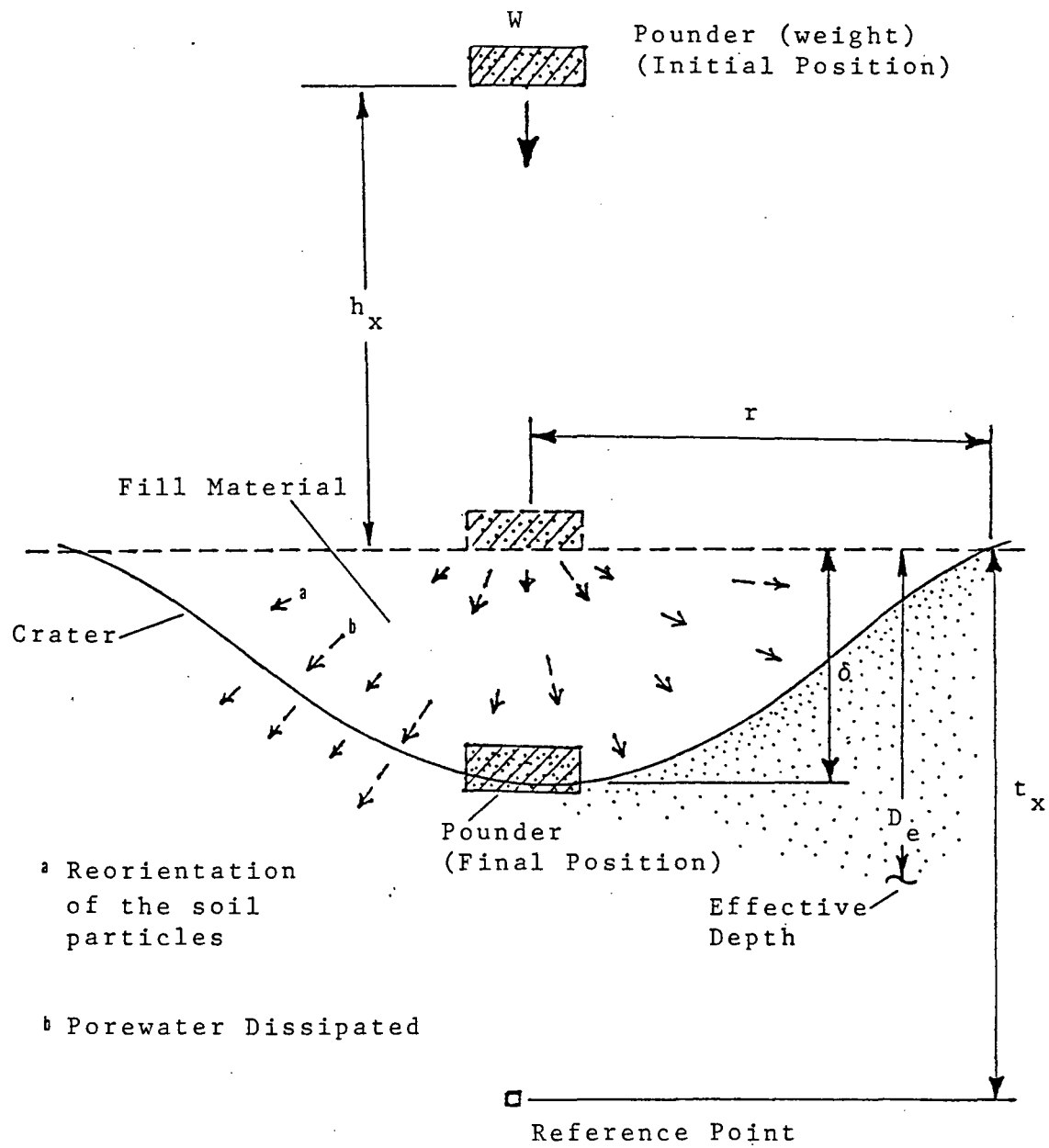


Figure 3 Schematic Diagram Illustrating the Soil-Pounder Interaction

3. LABORATORY EXPERIMENTAL STUDY

3.1 Material

Three distinct types of fill materials are used in this study: clay, sand and flyash (silt).

Clay: Silty clay with liquid limit equal to 29 and plasticity index equal to 5 was chosen with samples passed through a No. 10 sieve and air dried. The unified classification of this soil is denoted as ML-CL.

Sand: Uniform clean fine sand is used. The gradation for the sand is about 50% passing the No. 40 sieve and less than 1.0% passing the No. 200 sieve.

Flyash (silt): The flyash material was supplied by the Pennsylvania Power and Light Company of Martins Creek, Pennsylvania, with 58.7 percent of the flyash passing the No. 200 sieve and the several larger bottom-ash particles removed. All materials are air dried for the test. The gradation of these three types of fill material is shown in Fig. 4.

3.2 Test Equipment and Instrumentation

A metal drum 45.7 cm (18") in diameter and 57.6 cm (24") in height is used for this test (see Fig. 5). The clay foundation (see Fig. 5D) is about 25 cm (10") thick compacted by using standard AASHTO compaction on the silty clay obtained from the vicinity of Lehigh University.

Pressure Cell: The standard pressure cell with strain gauge is used for measuring the ground response due to the pounder. The strain gauge measures the deflection of the cell which is recorded on the oscillograph (see Figs. 5C and 6). The relationship between applied weight and oscillograph deflection was calibrated and found to be of a linear value of 0.1144 Newton (N) per

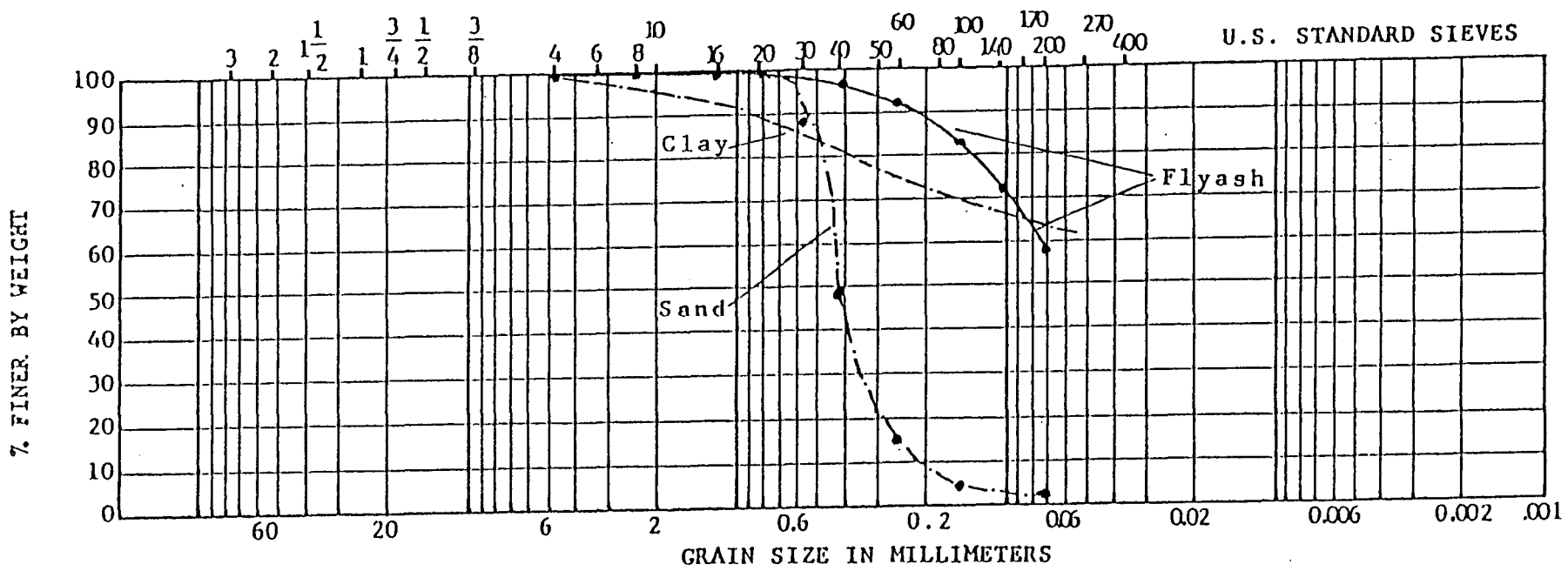


Figure 4 Grain Size Distribution of Clay, Sand and Flyash.

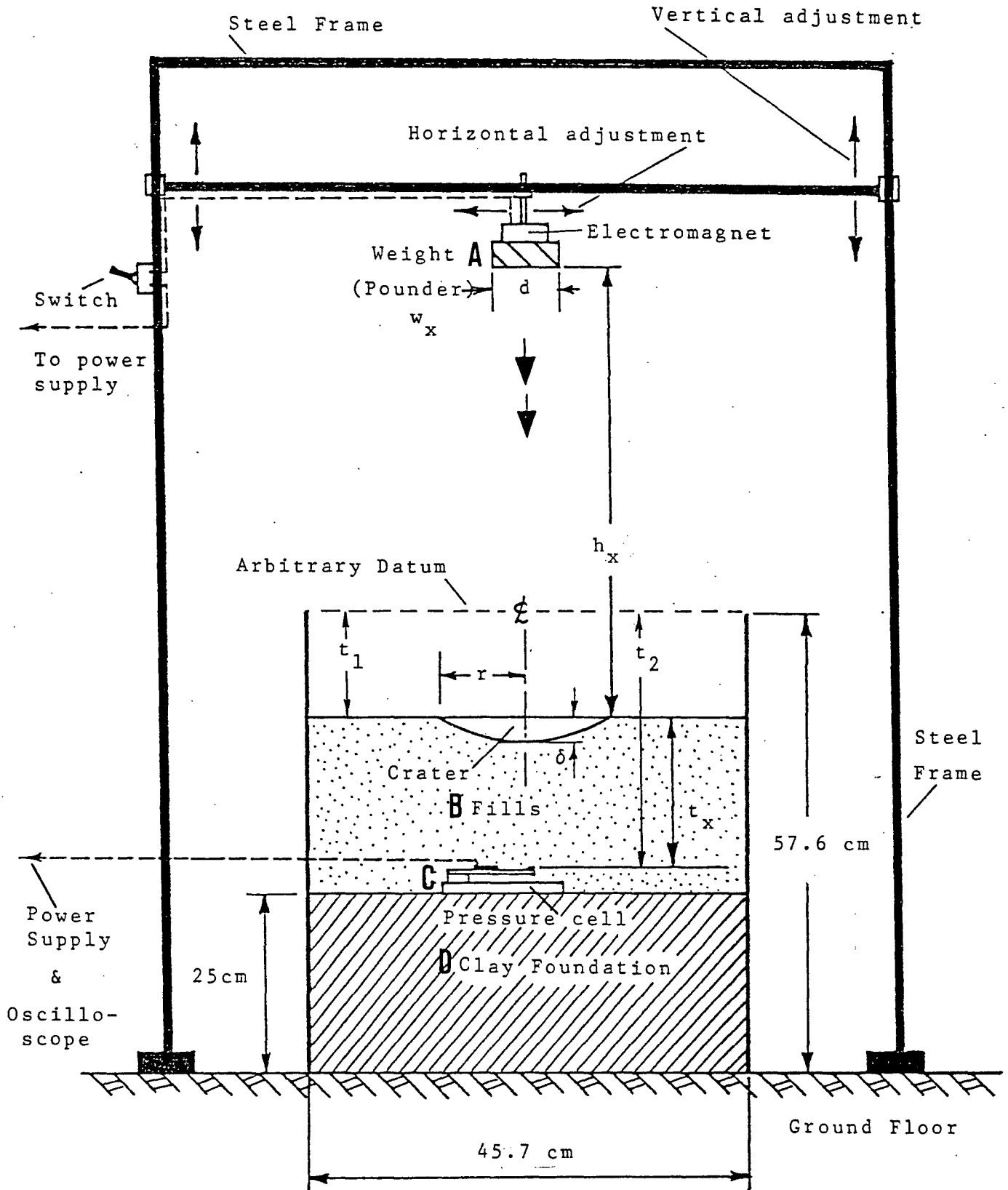


Figure 5 Laboratory Dynamic Densification Test

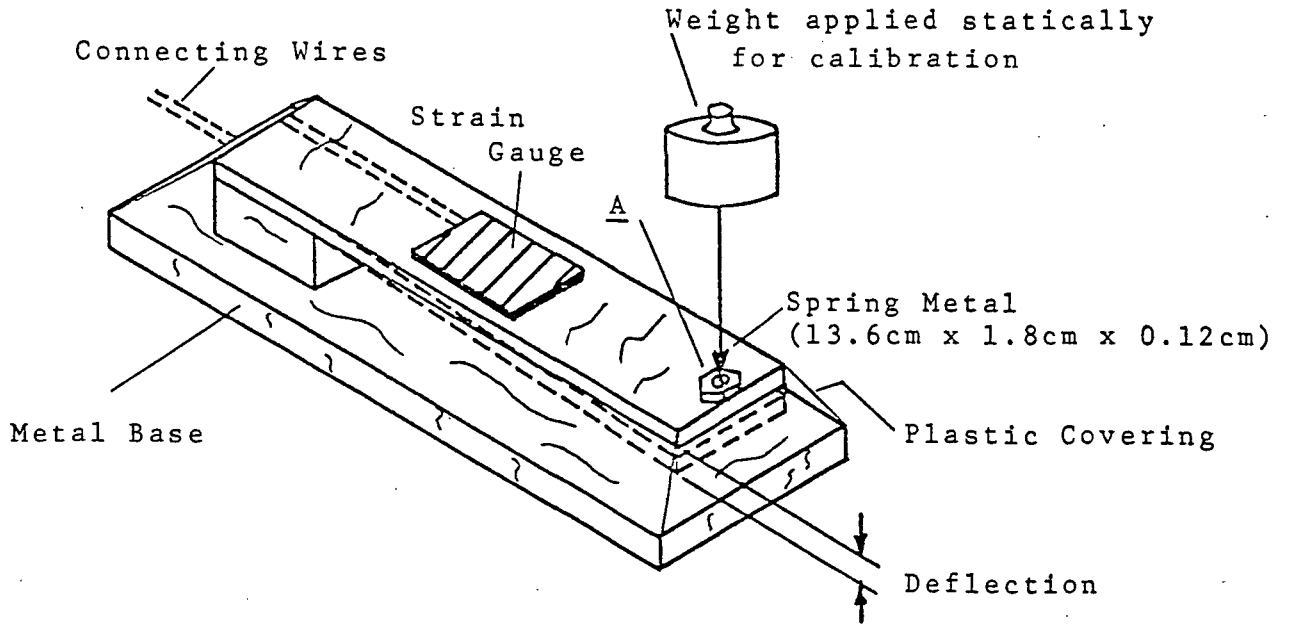


Figure 6 Ground Response Measuring Device During Dynamic Densification

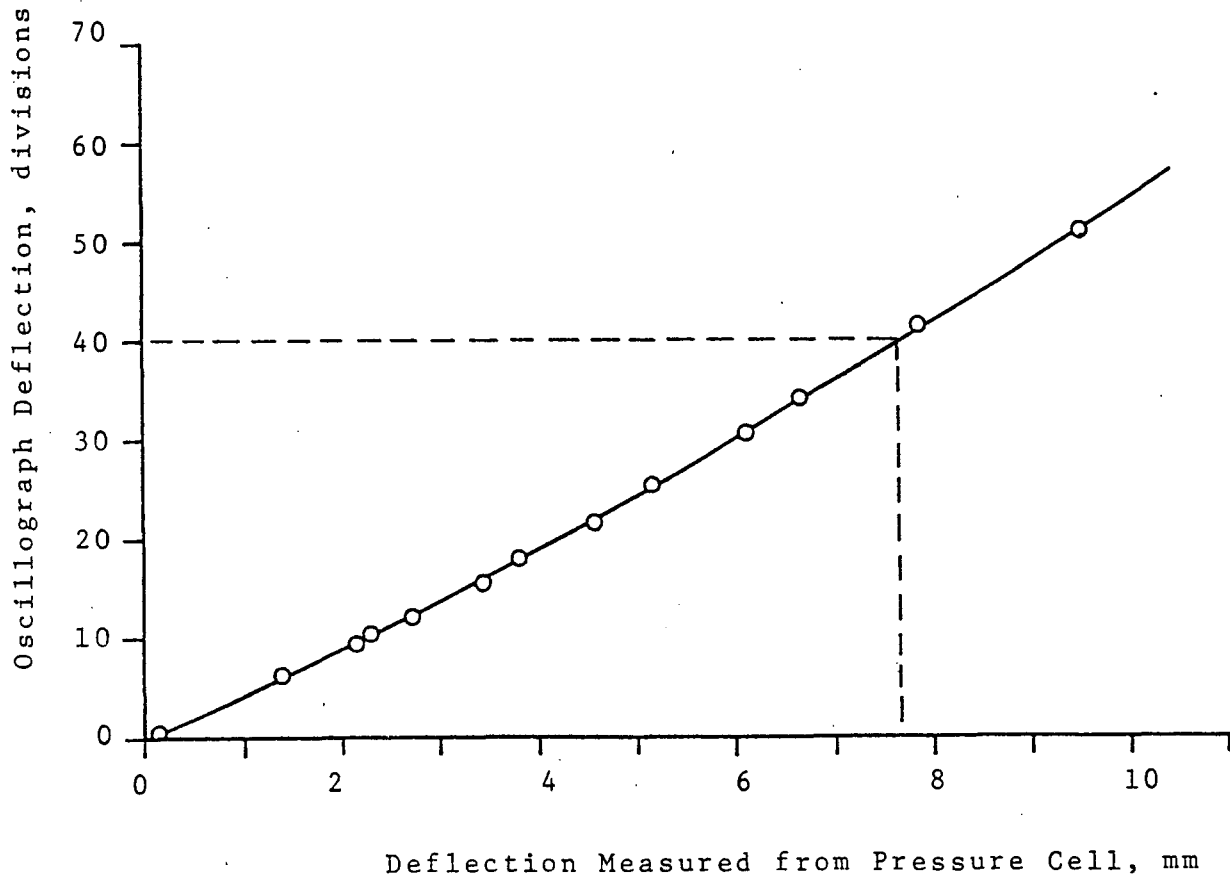


Figure 7 Calibration Chart for Oscillograph Deflection

oscillograph division. The oscillograph reading as related to the strain gauge deflection is also calibrated as shown in Fig. 7. The procedure for calibrating the pressure cell is to apply various known weights statistically at point A in Fig. 6 and then correlating this weight with the oscillograph deflection.

Drop Weight (Pounder): The weights used for this study were made from hard steel plate. The plate is thick enough to resist bending during the test. The weight of the pounder is denoted as w_x and the diameter is denoted as d as shown in Fig. 5A. Four diameters varying from 3.2 cm to 10.0 cm are used. The pounder area varies from 8.07 cm² to 78.5 cm². To control the drop of the pounder, an electromagnet system is used as shown in Fig. 5A.

3.3 Test Procedure

Control of Drop Weight (Pounder): An electromagnetic system is connected with the pounder (see Fig. 5A). To release the weight, the switch to the electromagnet is turned off, at the same time the oscillograph is turned on to measure the ground response by measuring the force from the strain gauge on the pressure cell. After the weight is dropped, the oscillograph is turned off and the pounder is carefully removed from the crater as shown in Fig. 5B. This process is repeated six times as described in a later section of this report. After the sixth reading, the oscillograph deflections are measured from the strip charts (see Figs. 8 and 9). The value is measured as the distance from the pre-drop reading to the peak (maximum) deflection, then multiplying this value by the calibration factor and averaging the six results yields the average ground response in Newtons (N).

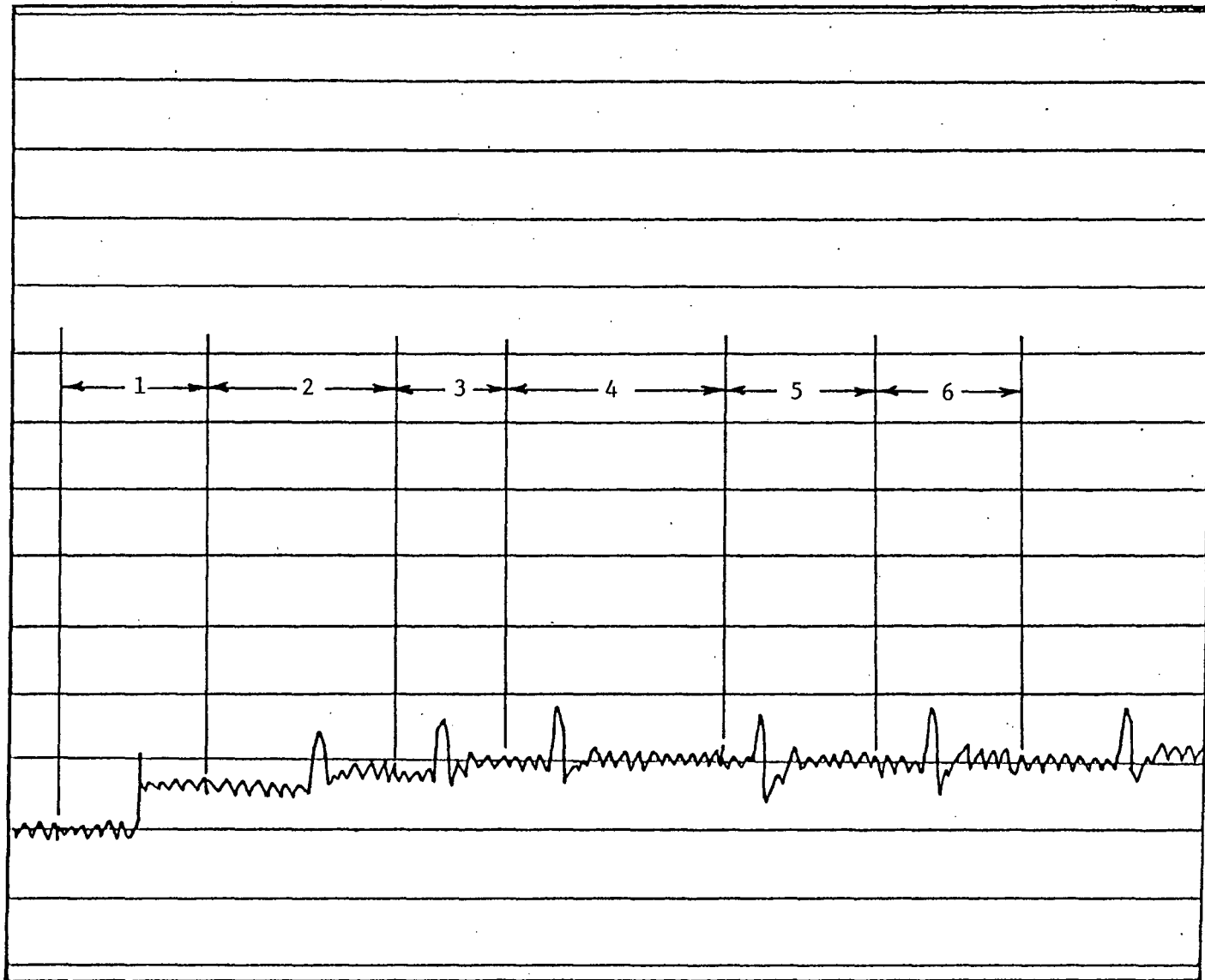


Figure 8 Typical Ground Response of Fill Material for Large Overburden Depths Measured from Oscillograph Chart

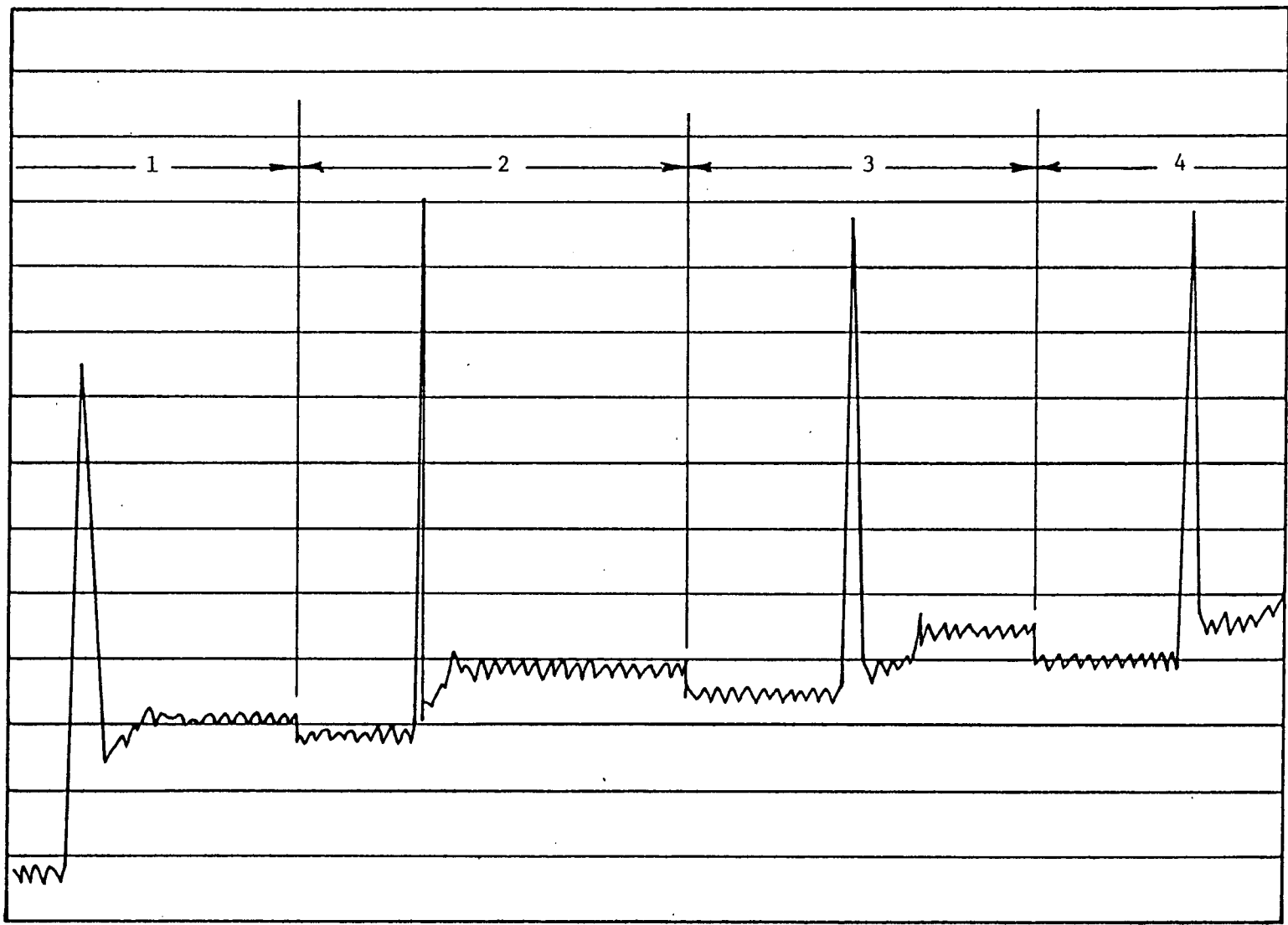


Figure 9 Typical Ground Response of Fill Material for Small Overburden Depths Measured from Oscillograph Chart.

Height of Drop, h_x , and Overburden Depth, t_x : The datum line shown in Fig. 5B is arbitrarily selected. The vertical distance, t_2 , from the datum to the strain gauge can be measured in two ways:

(1) for small overburden (fill) depths, the mechanical pointer (see Fig. 10) on the mounted callipers is pushed through the fill until it reaches the strain gauge. At this point, the oscillograph reading will change and the vertical distance can be read from the callipers.

(2) when the overburden (fill) depths become greater, a second method must be used. Before adding the fill, the depth to the gauge from the datum and corresponding oscillograph reading are found by the first method. The gauge deflection caused by the addition of fill is measured on the oscillograph. The additional depth to the gauge is then read from the deflection calibration curve and added to the previously calculated depth to find t_2 . The distance, t_1 , from the datum to the soil surface directly above the gauge is measured using the mounted callipers. Subtracting t_1 from t_2 gives the depth of fill, t_x .

Crater Profile Measurements: A depression crater is caused by the densification process. It is varied by the poulder area, densification energy and material types. To examine the characteristics of the crater profile, the following measuring techniques are used. The overall picture of a crater profile after each weight is dropped is shown in Fig. 5B. Typical profiles of clay, sand, and flyash are shown in Figs. 21 to 26 respectively.

The profiles are measured for each drop with each poulder size and material type. Before the weight is dropped, the surface material is leveled. The

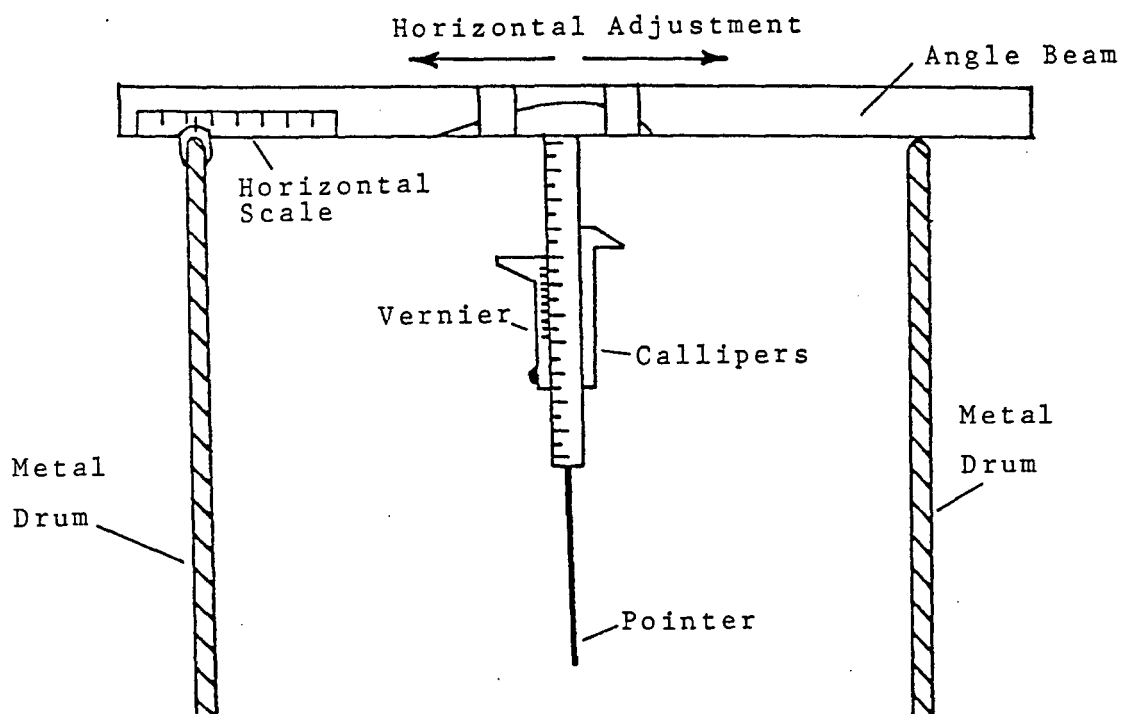


Figure 10 Mechanical Mounted Callipers for Measuring Ground Profile after Dynamic Densification

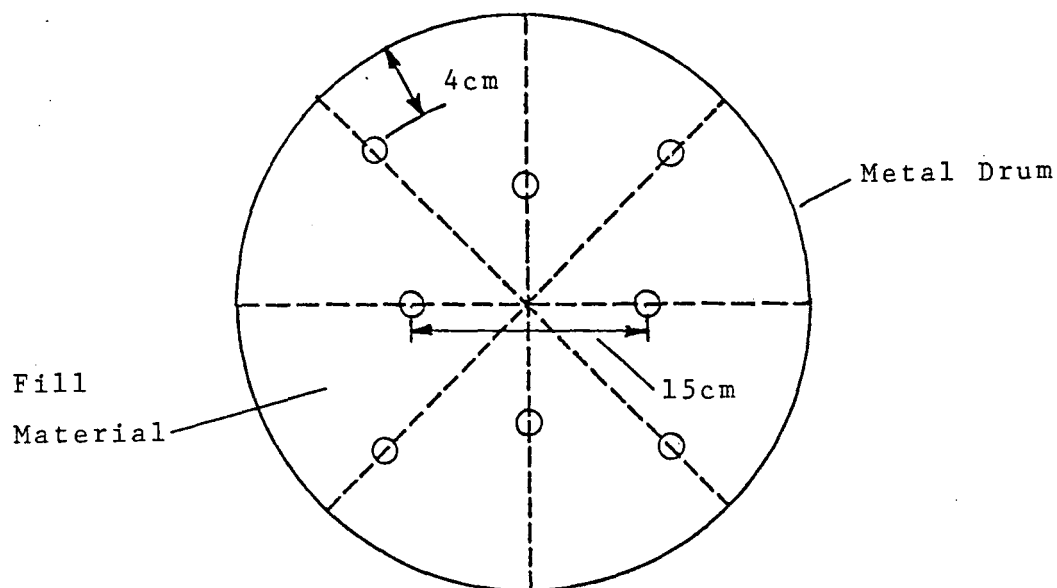


Figure 11 Top View of Locations for Measuring the Depth of Fill in order to Calculate the Unit Weight of Overburden Fill Material.

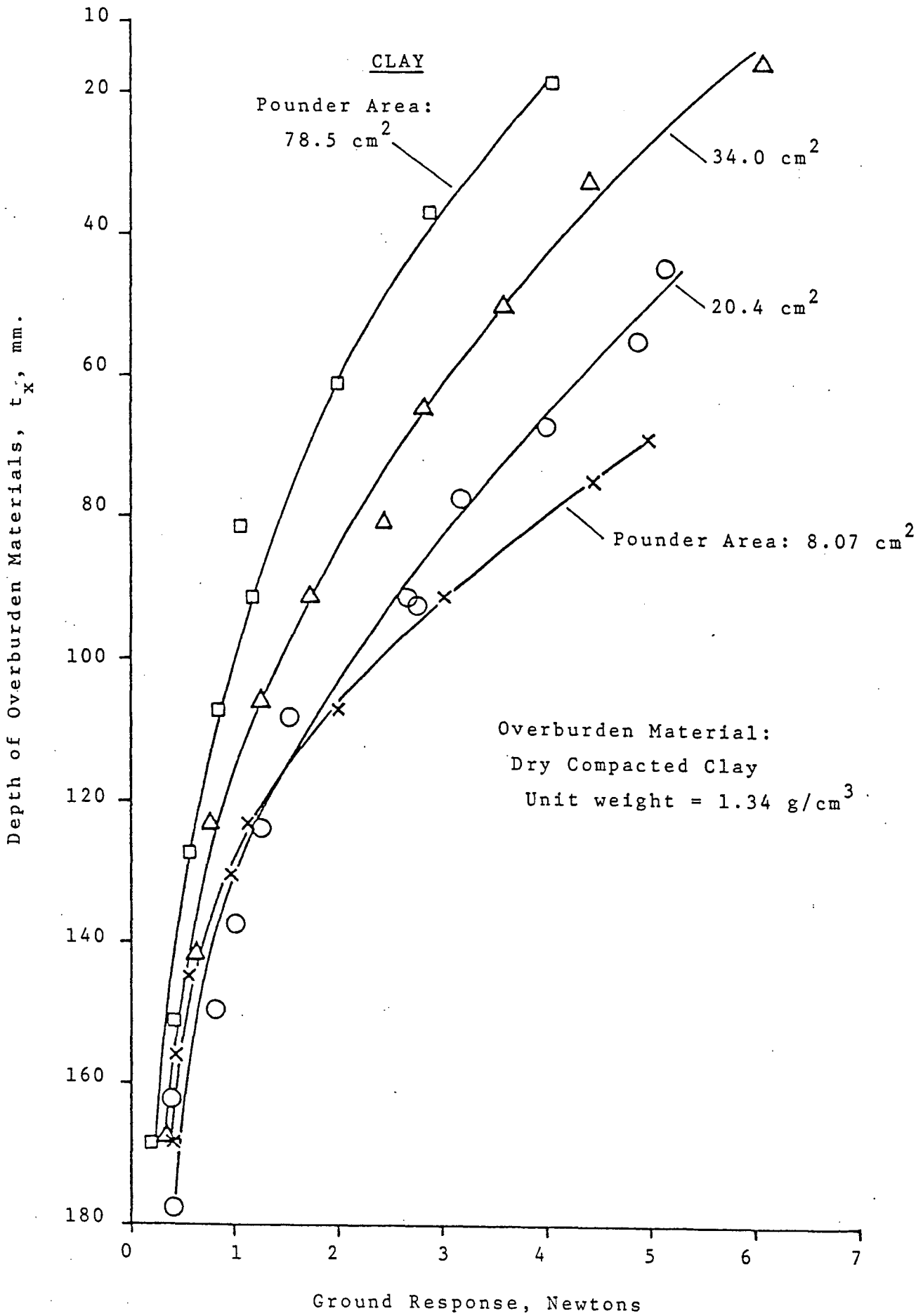


Figure 12 Effect of Overburden Depth on Ground Response

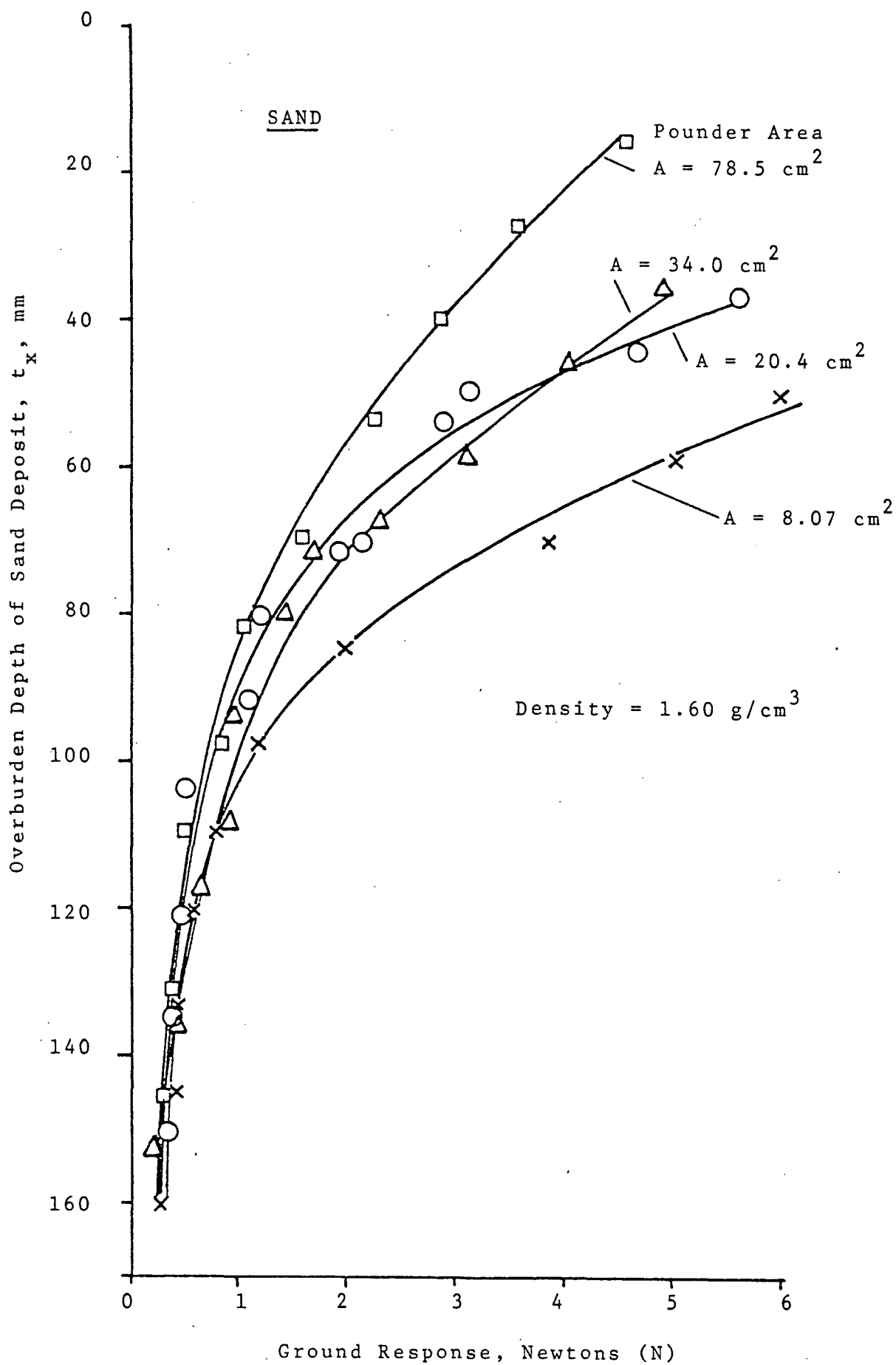


Figure 13 Effect of Overburden Depth on Ground Response

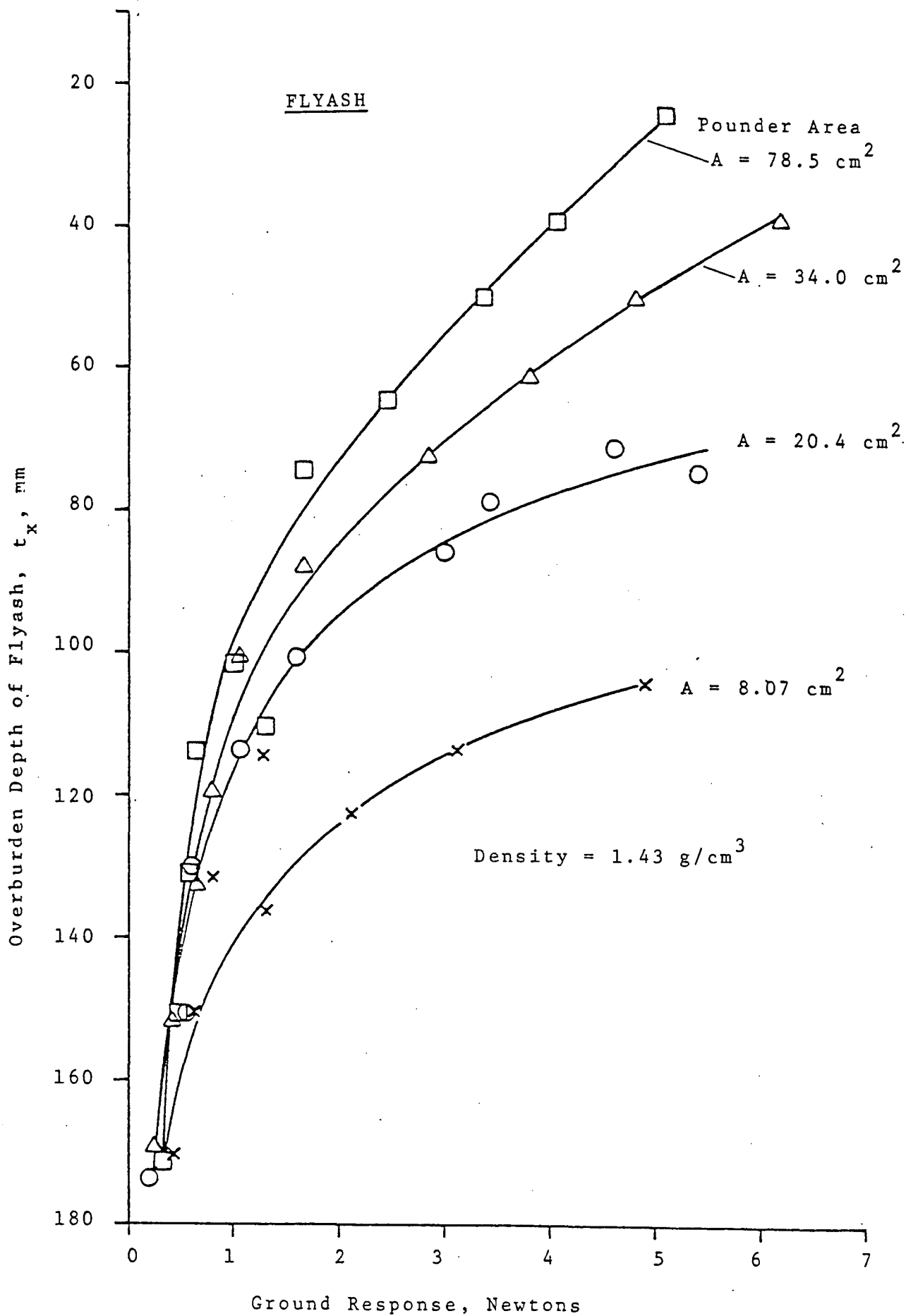


Figure 14 Effect of Overburden Depth on Ground Response

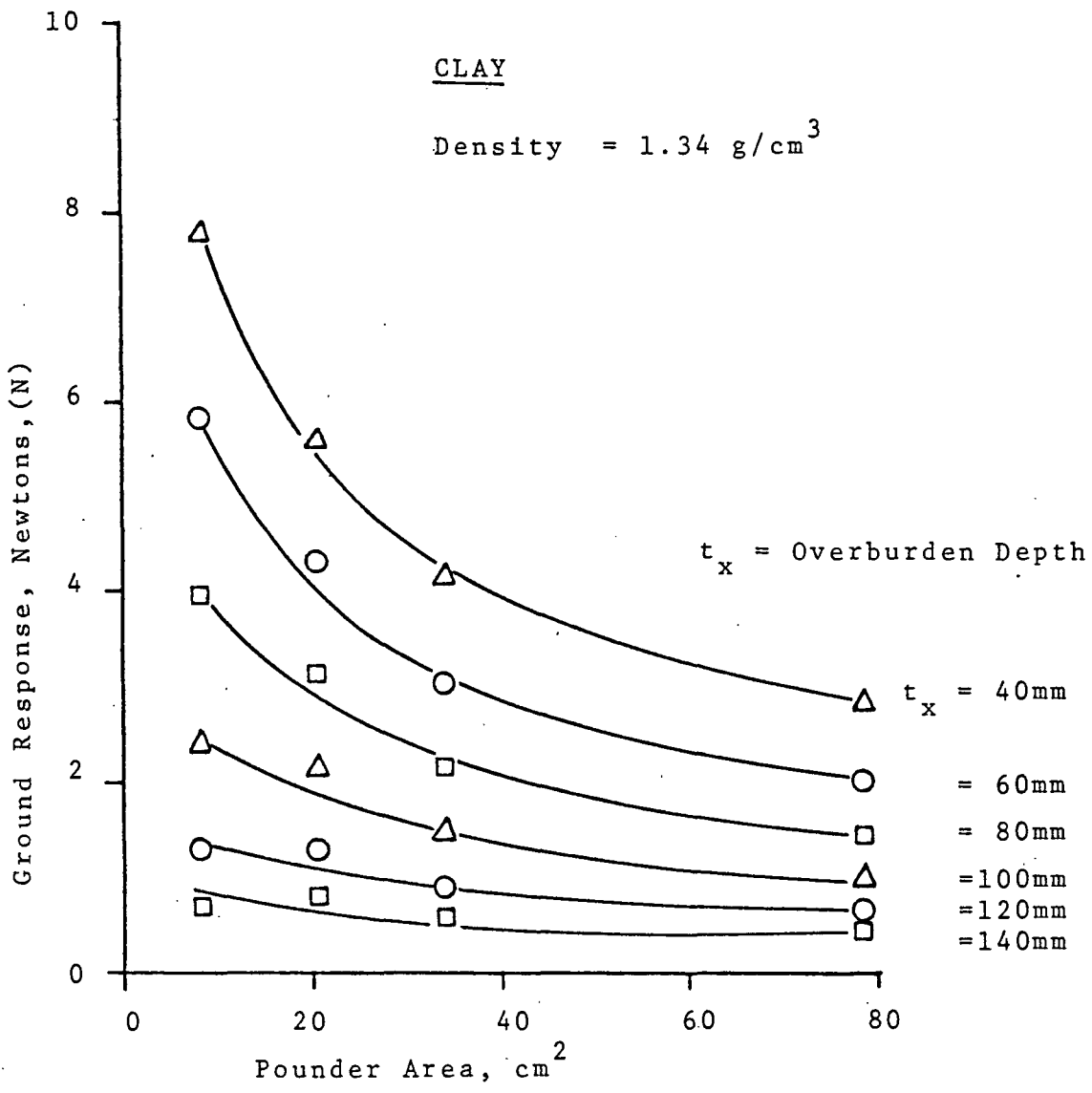


Figure 15 Ground Response versus Pounder Area with Various Depths of Clay

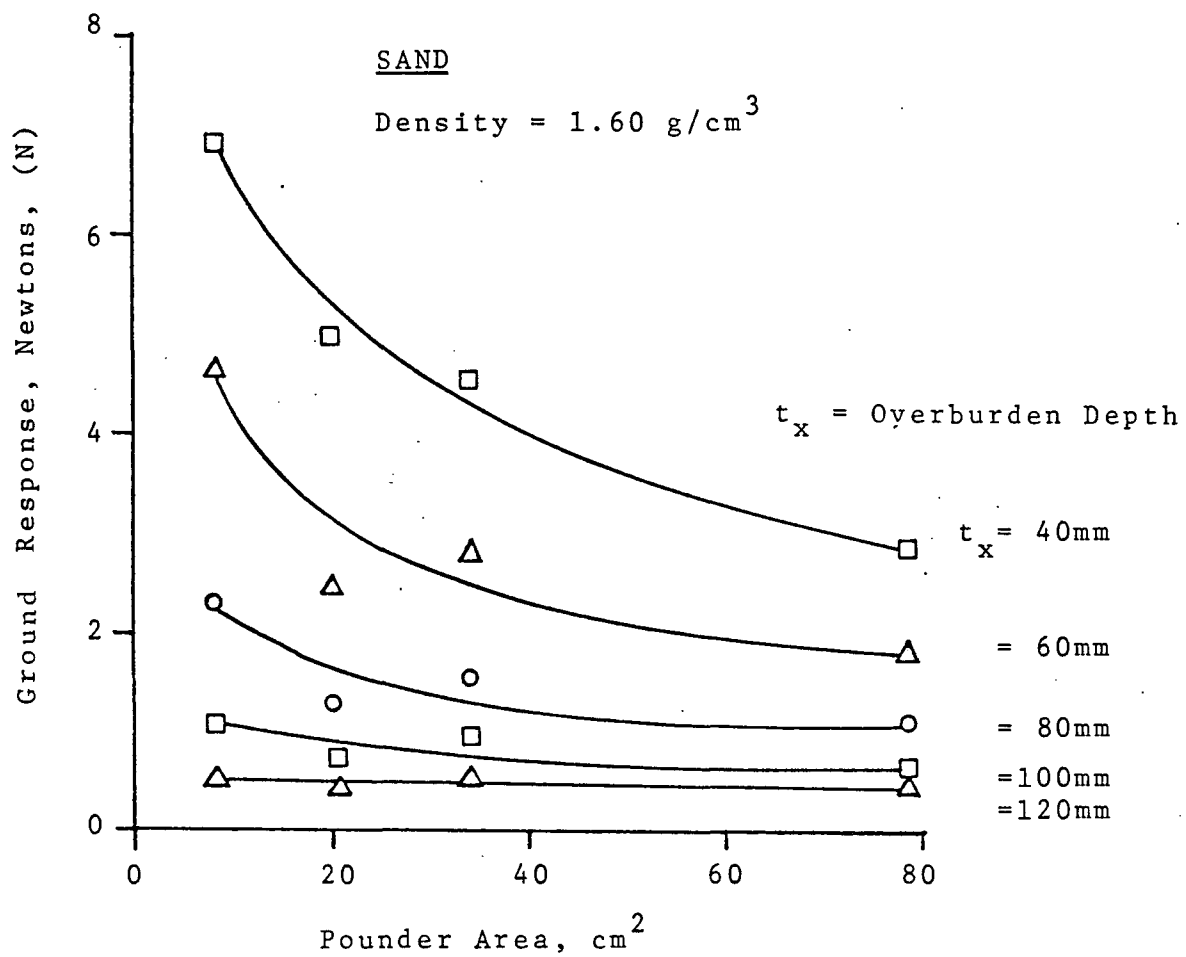


Figure 16: Ground Response versus Pounder Area with Various Depths of Sand

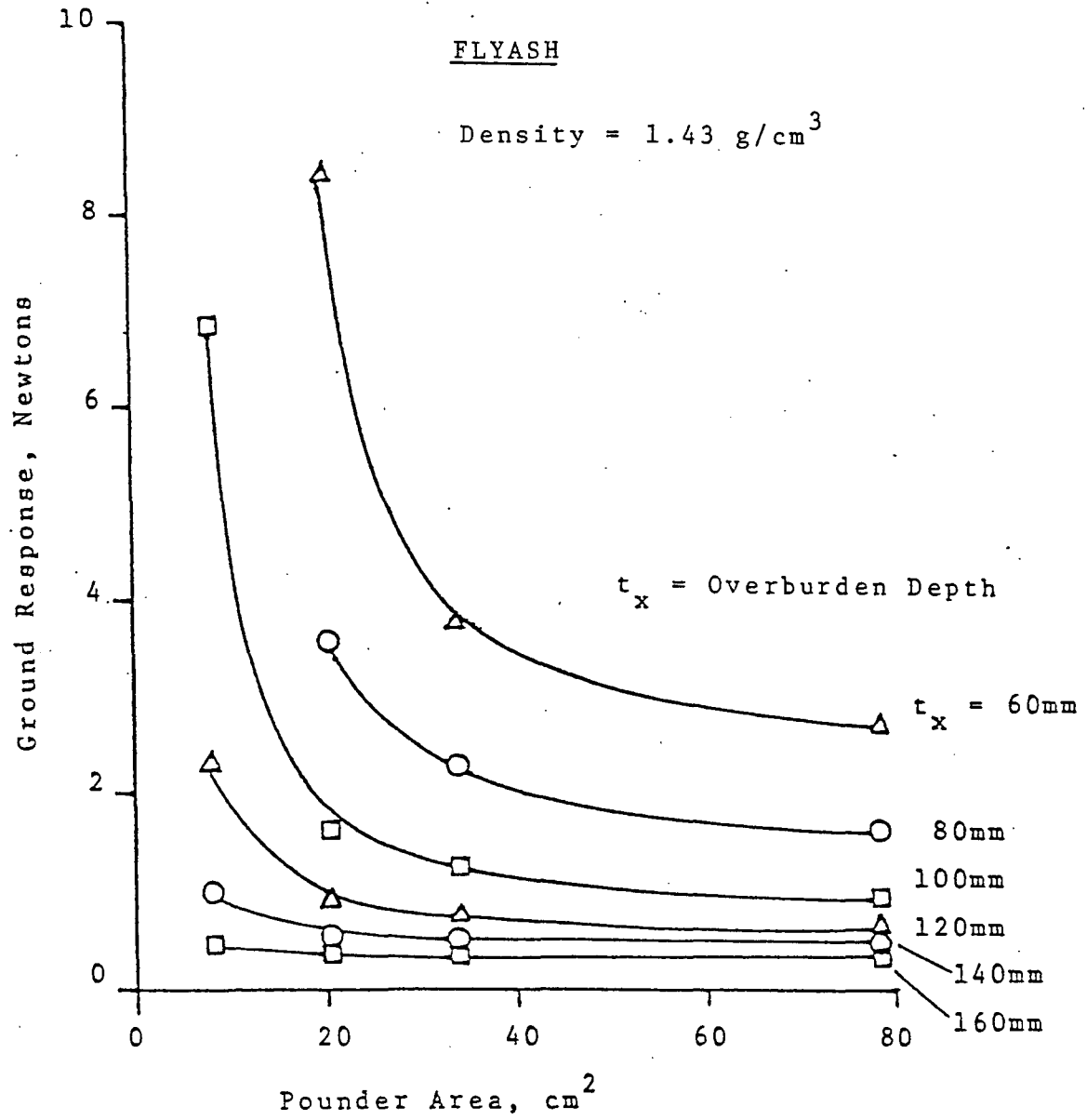


Figure 17 Ground Response versus Pounder Area with Various Depths of Flyash

distance from the datum to the undisturbed surface is denoted as t_1 and is measured at 2 cm intervals across the expected crater area. After each of the six drops, the distance from the datum to the surface of the crater profile ($t_1 + \delta$) is measured. Also, the horizontal points at the crater's edge and the horizontal location and depth of the deepest point of the crater are recorded (see Fig. 27). Crater areas and volumes are computed and plotted versus poulder areas for all three fill materials as presented in Figs. 27 and 29.

Density of Fill: Before the fill is added, measurements are made from the datum to eight (8) random points on the clay foundation (Fig. 4D). Then the fill is added and several trials are run. The surface is leveled and measurements are made from the datum to the surface at the same eight (8) points (see Fig. 11). Subtracting the values gives the fill depth. The average depth is calculated and with the diameter of the metal drum (45.7 cm), the volume of fill can be computed. Dividing the mass of fill added by the volume of fill added yields the unit weight (density) of the fill material.

4. SUMMARY OF TEST RESULTS AND DISCUSSION

4.1 Thickness of Fill and Poulder Area

Thickness of fill versus ground response with various poulder areas and constant densification energy are summarized for all three fill materials in Figs. 12 to 14. The thickness, t_x , varies from 20 mm to 175 mm. Four poulder areas are used varying from 8.07 cm² to 78.5 cm². The ground response is the force acting on the pressure cell in Newtons (N). It is obvious that for a

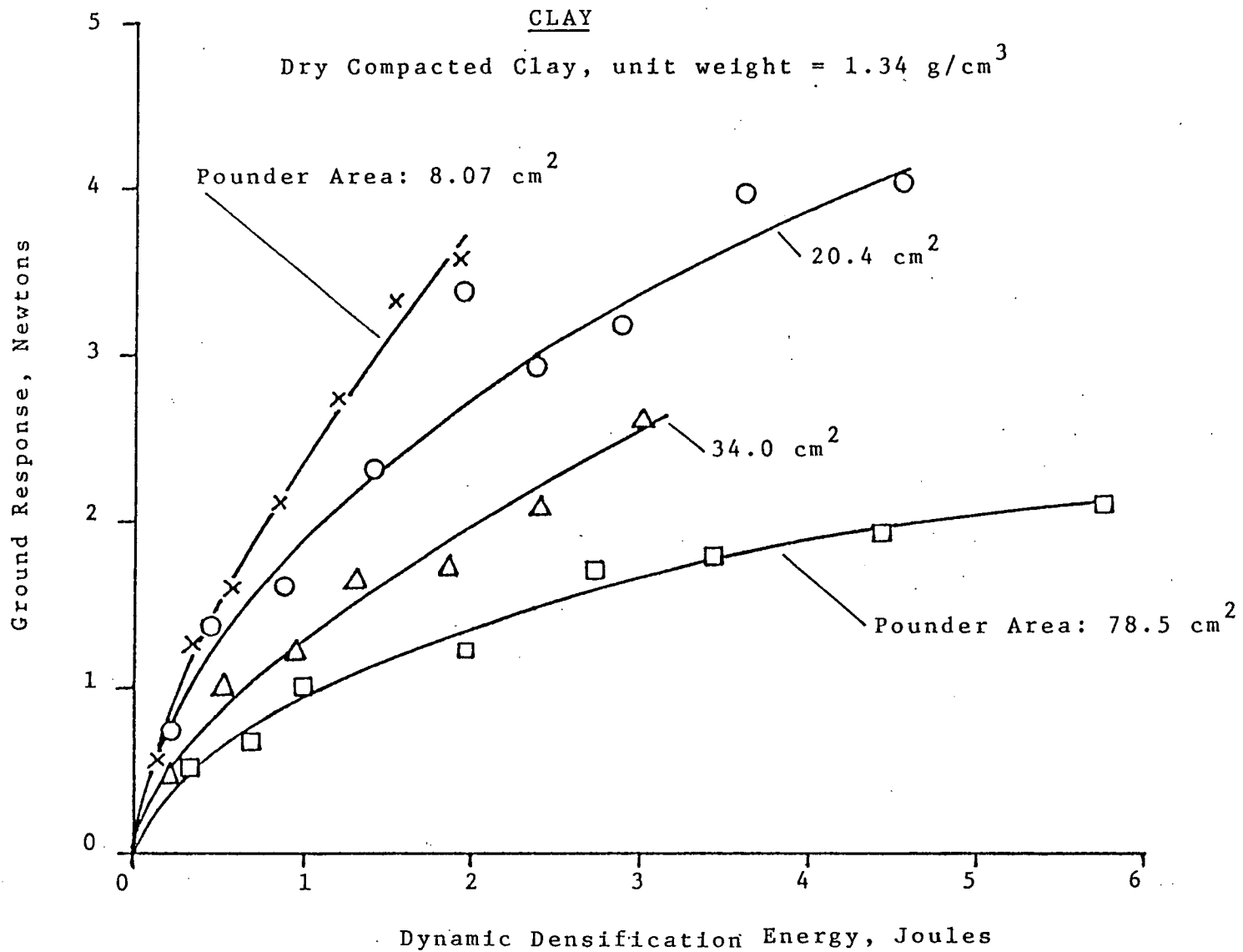


Figure 18 Soil Response Caused by Dynamic Densification with Various Pounder Areas at Depth of Overburden = 80 mm

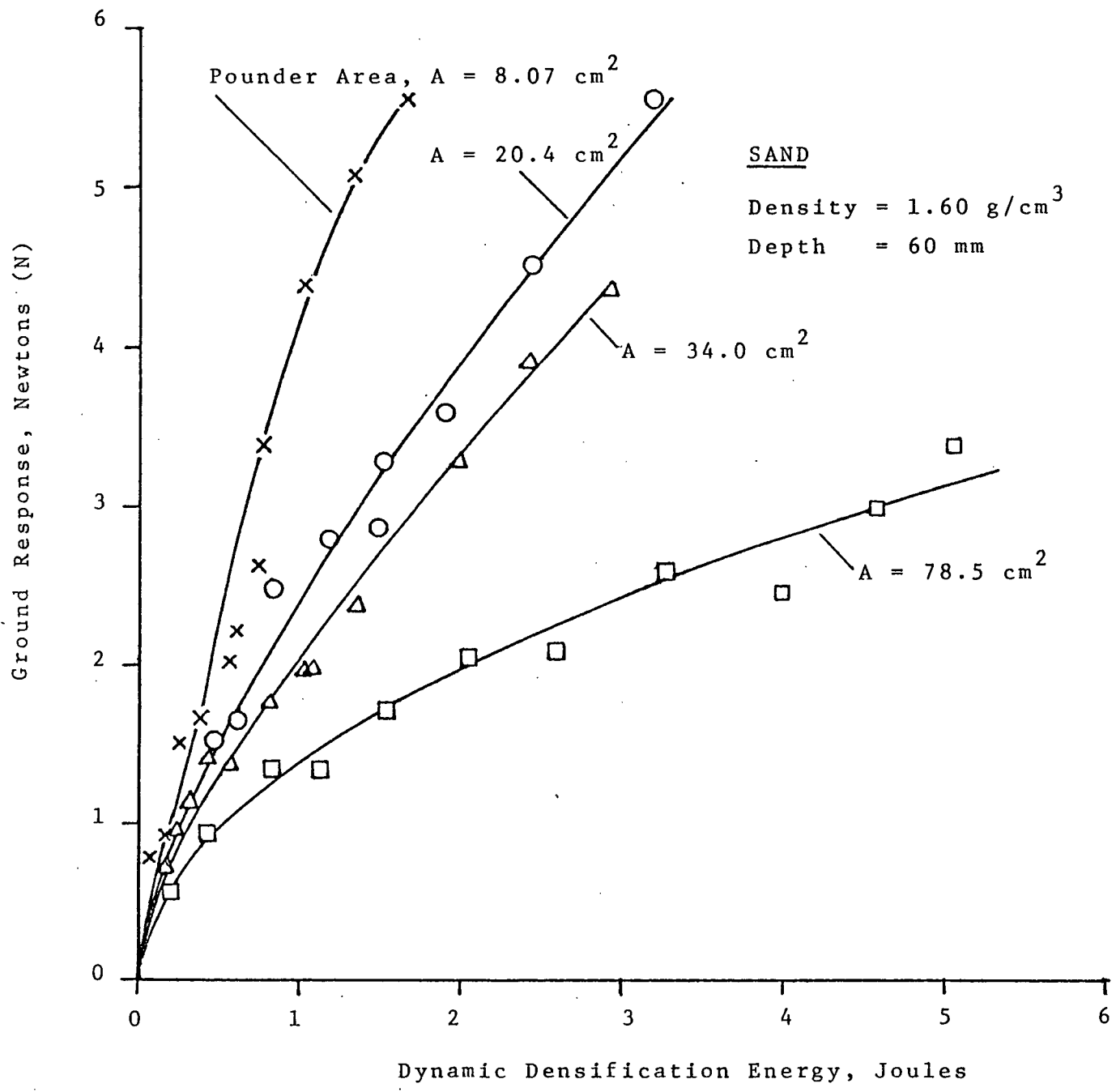


Figure 19 Sand Response Caused by Dynamic Densification with Various Pounder Areas at Depth of Overburden = 60 mm.

FLYASH

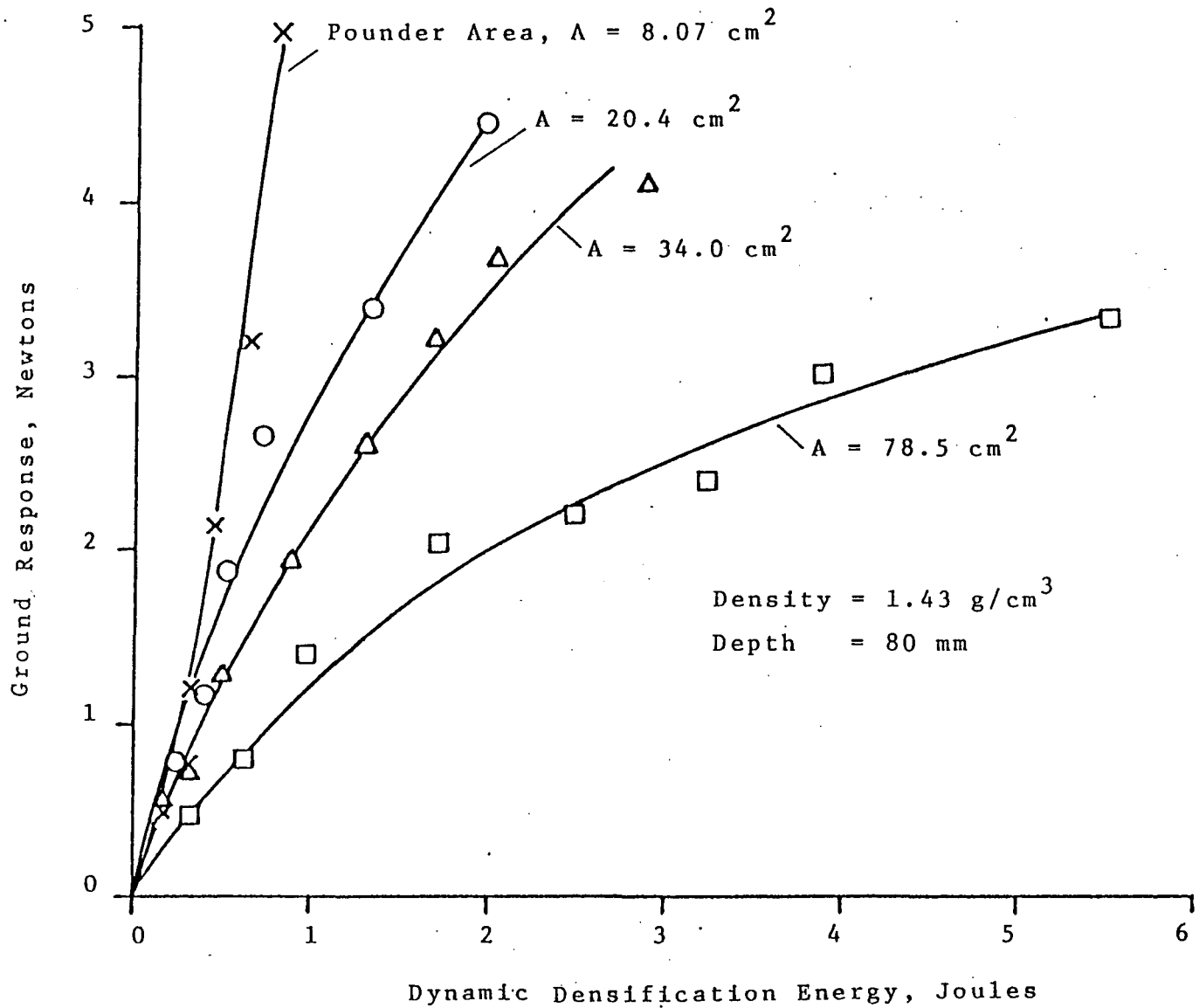


Figure 20 Flyash Response Caused by Dynamic Densification with Various Poulder Areas at Depth of Overburden = 80 mm.

thin layer deposit the ground response is higher, and this is true for all poulder sizes.

In comparing the response of the three types of soils, the flyash clearly has a greater response at shallow depths. The shapes of the ground response curves show a similarity between the flyash and sand when compared with the response of the clay. Both the flyash and sand have high ground responses at shallow depths followed by a rapid reduction in the response with depth. The clay response, however, is less at shallow depths but reduces more gradually allowing for more response at greater depths.

Figs. 15 to 17 are interpreted from Figs. 12 to 14 showing that for the thin deposit (say $t_x = 60$ mm), the poulder size has significant effect on ground response. This is particularly true of flyash where for each overburden depth shown, the ground response increases rapidly at a critical poulder size. However, for the thicker layer ($t_x = 160$ mm), the poulder size has little effect on the ground response. Also indicated in these figures, the larger the poulder area, the less effect on the ground response for all three fill materials, clay, sand and flyash.

4.2 Ground Response and Densification Energy

Ground response versus dynamic densification energy for clay, sand and flyash are presented in Figs. 18 to 20. The densification energy, E , is equal to the weight of poulder, w_x , times the drop height, h_x , expressed as:

$$E = w_x h_x \quad (3)$$

For variable densification energy, the height of the drop, h_x , is adjusted by moving the cross-bar up or down on the steel frame to the desired height as the pounder is lined directly above the strain gauge of the pressure cell. Theoretically, the densification energy can be estimated from Eq. (3); however, densification behavior is also influenced by pounder size and shape, fill material types, lower layer ground foundation characteristics, degree of saturation, etc. As indicated in Figs. 18 to 20, the higher the densification energy, the greater the ground response for all pounder sizes and weights for all three fill materials. However, the ground response for smaller pounder areas ($A = 8.07 \text{ cm}^2$) is more sensitive to the densification energy than for larger pounder areas ($A = 78.5 \text{ cm}^2$).

4.3 Crater Profiles

A depression crater is caused by the densification process. The shape of the crater is influenced by pounder area, number of drops, fill material types, and densification energy. Figures 21 to 26 present the typical crater profiles for various fill materials with two pounder areas, $A = 8.07 \text{ cm}^2$ and $A = 78.5 \text{ cm}^2$. Number of drops, n , varied from 1 to 6 with drops 1, 2, 3 and 6 indicated in the figures. These figures clearly show that for the clay the surface area is small, but the depth is greater. However, for the flyash the surface area is greater but the depth is less. For the larger pounder area ($A = 78.5 \text{ cm}^2$), the profiles show an entirely different shape when compared with the smaller pounder areas. For small pounder areas the crater can be approximated by an inverted cone while for large pounder areas the profile can be approximated by a trapezoid. Also, for the sand it is shown that heave occurs at the edge of the crater. No heave is recorded for both clay and flyash fills.

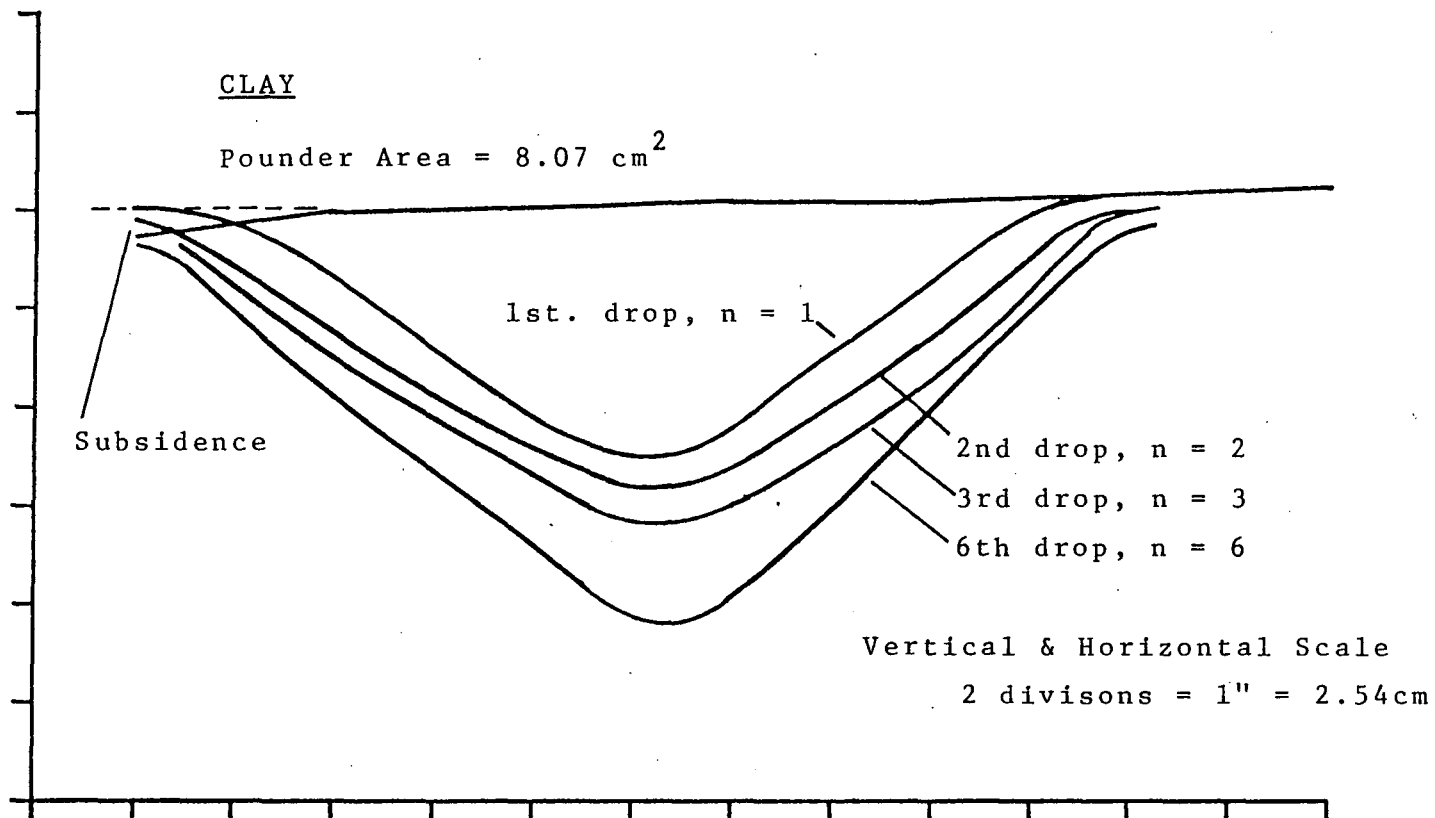


Figure 21. Effect of Pounder Area and Number of Drops on the Shape of Crater Cross-section of Clay Fill.

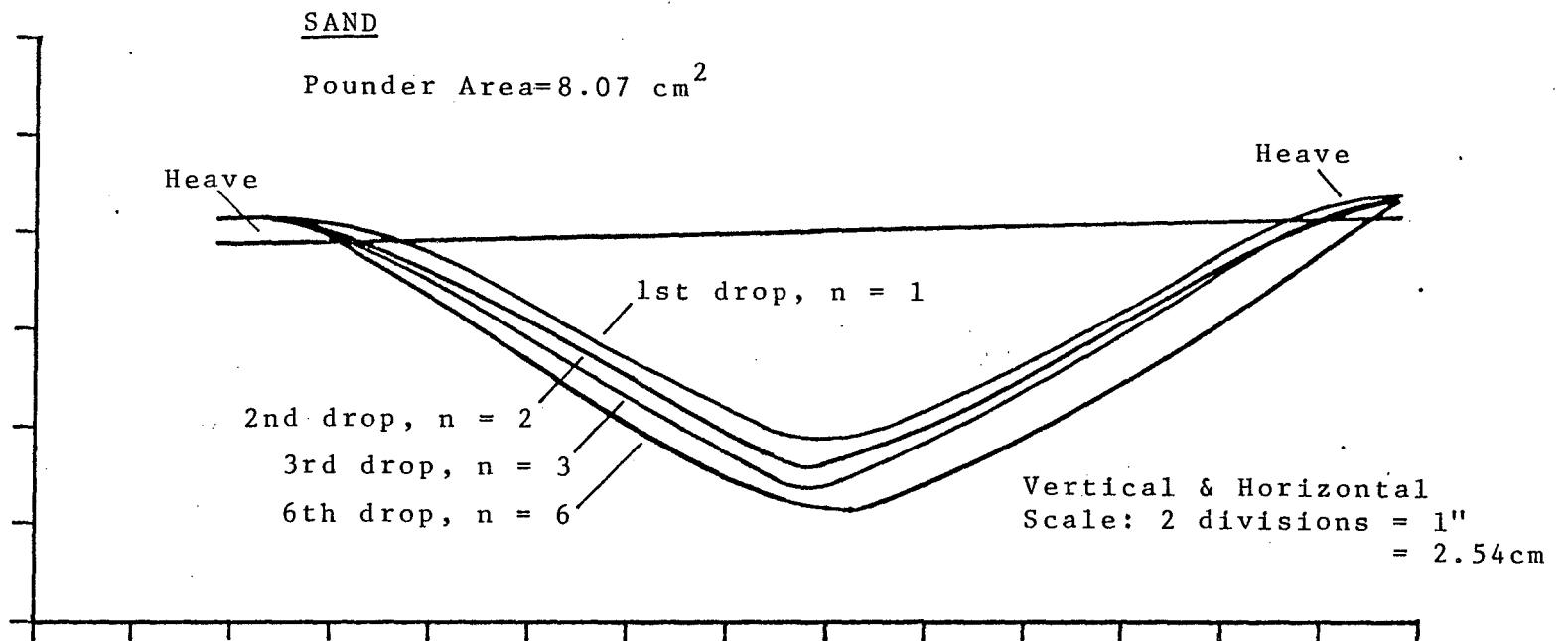


Figure 22 Effect of Pounder Area and Number of Drops on the Shape of Crater Cross-section of Sand Fill.

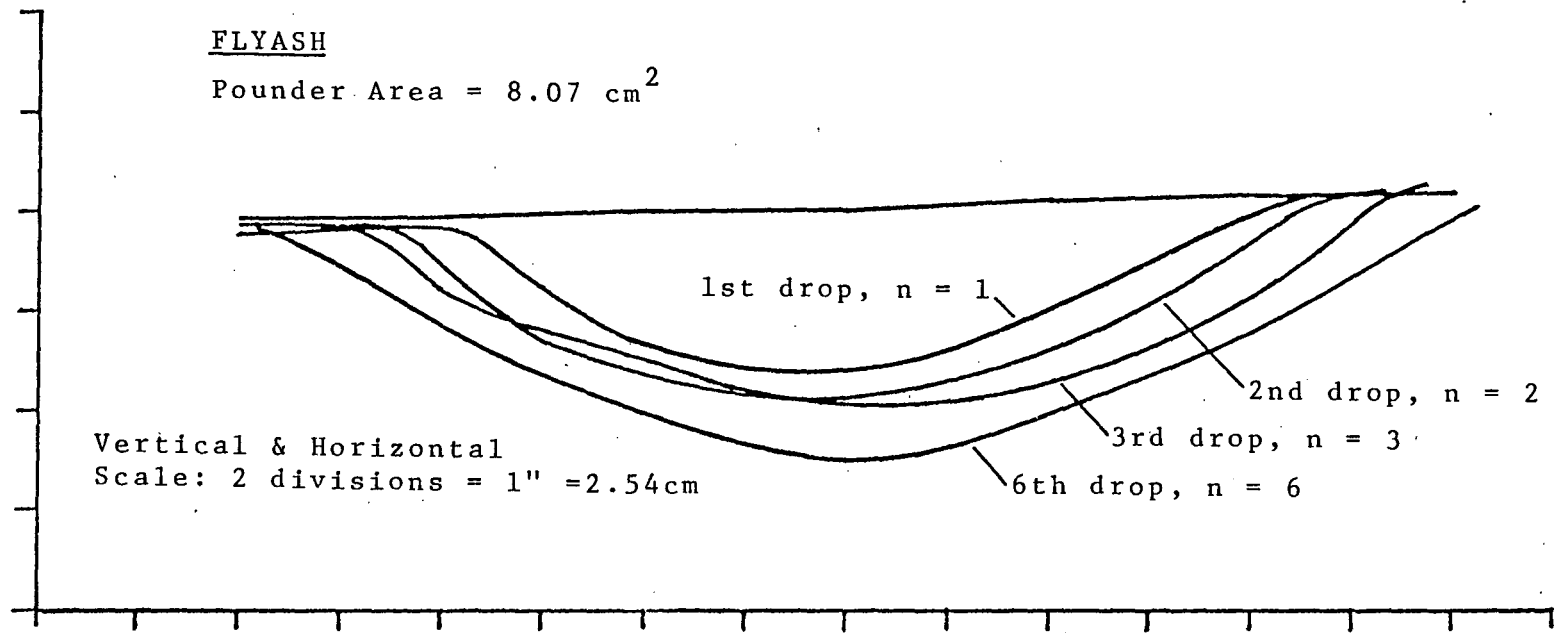


Figure 23 Effect of Pounder Area and Number of Drops on the Shape of Crater Cross-section of Flyash Fill.

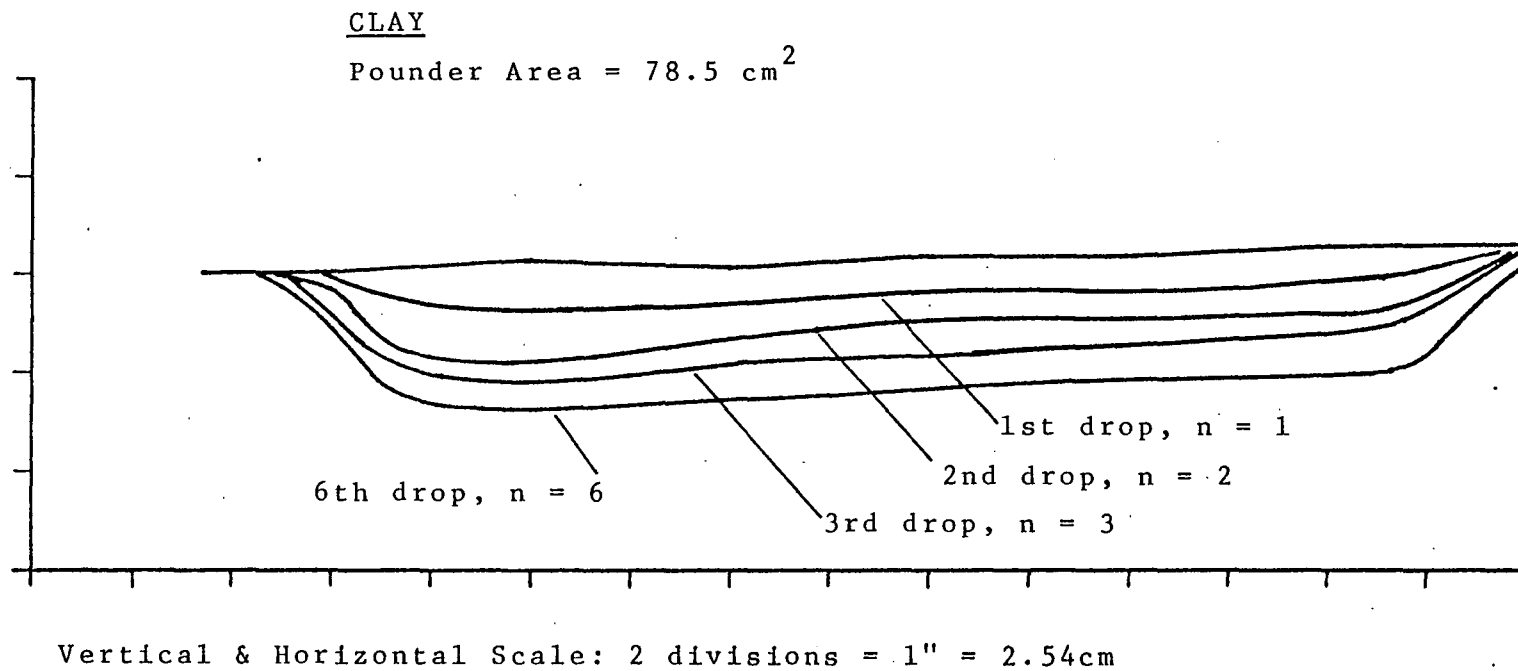


Figure 24 Effect of Pounder Area and Number of Drops on the Shape of Crater Cross-section of Clay.

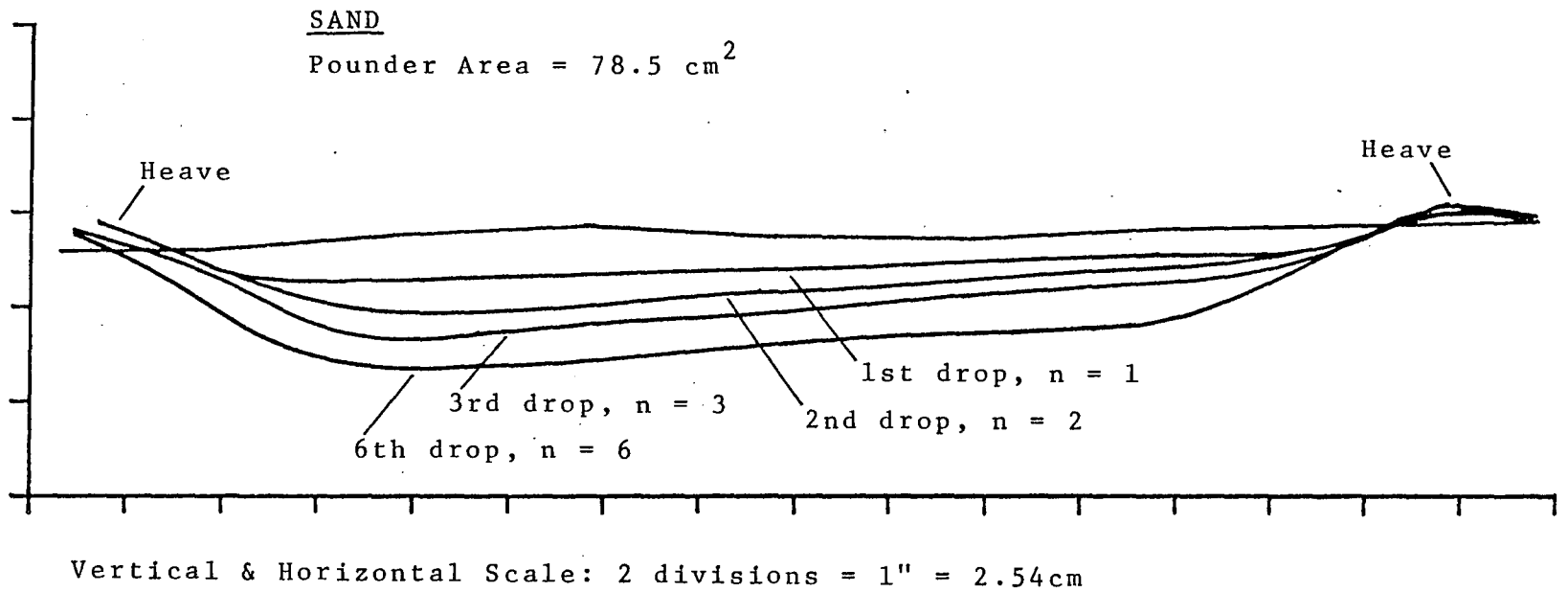


Figure 25 Effect of Pounder Area and Number of Drops on the Shape of Crater Cross-section of Sand Fill.

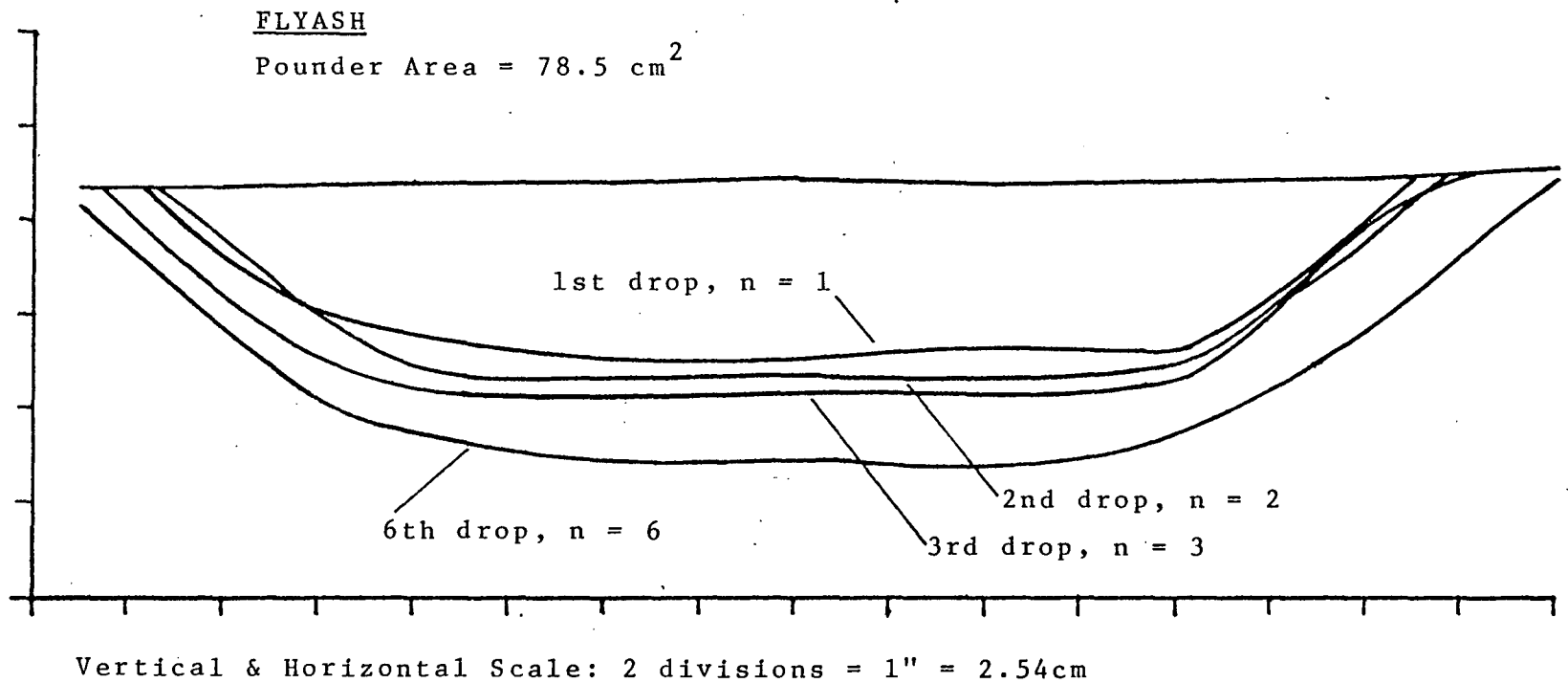


Figure 26 Effect of pounder Area and Number of Drops on the Shape of Crater Cross-section of Flyash Fill.

4.4 Crater Area and Volume

Based on the data from Figs. 21 to 26 and the maximum depth of the crater, the surface areas of the crater and volumes of the crater versus poulder areas with constant densification energy for various fill materials are obtained as shown in Figs. 27 to 29. The crater volume is computed based on a conical shape as shown in Eq. (4):

$$v = \frac{1}{3} \pi r^2 \delta \quad (4)$$

where δ , is the deepest crater depth and r , is the crater radius after 6 drops. For larger poulder sizes the crater volume calculated by this equation is less than the actual value because the crater shape is no longer conical.

It is indicated clearly that the flyash gives greater crater areas and volumes than sand and clay. For the smaller poulder area, the crater area is small, and the crater area increases as the poulder area increases. However, after the poulder area reaches a certain size ($A = 34.0 \text{ cm}^2$), the crater creates the side-slip phenomena after the poulder is removed. For the sand, the side-slip phenomena has greater effect in comparison with flyash and clay.

4.5 Number of Drops, n

Further plotting of crater radius and deformation-height of drop ratios versus the number of drops, n , are presented in Figs. 30 and 31. Figure 31 shows the crater depth-height of drop ratio increases as the number of drops, n , increases for all three fill materials. The ratio is much higher for flyash than it is for sand and clay. The rate of increase for the clay and flyash is greater than sand. The ratio of radius-height of drop versus number

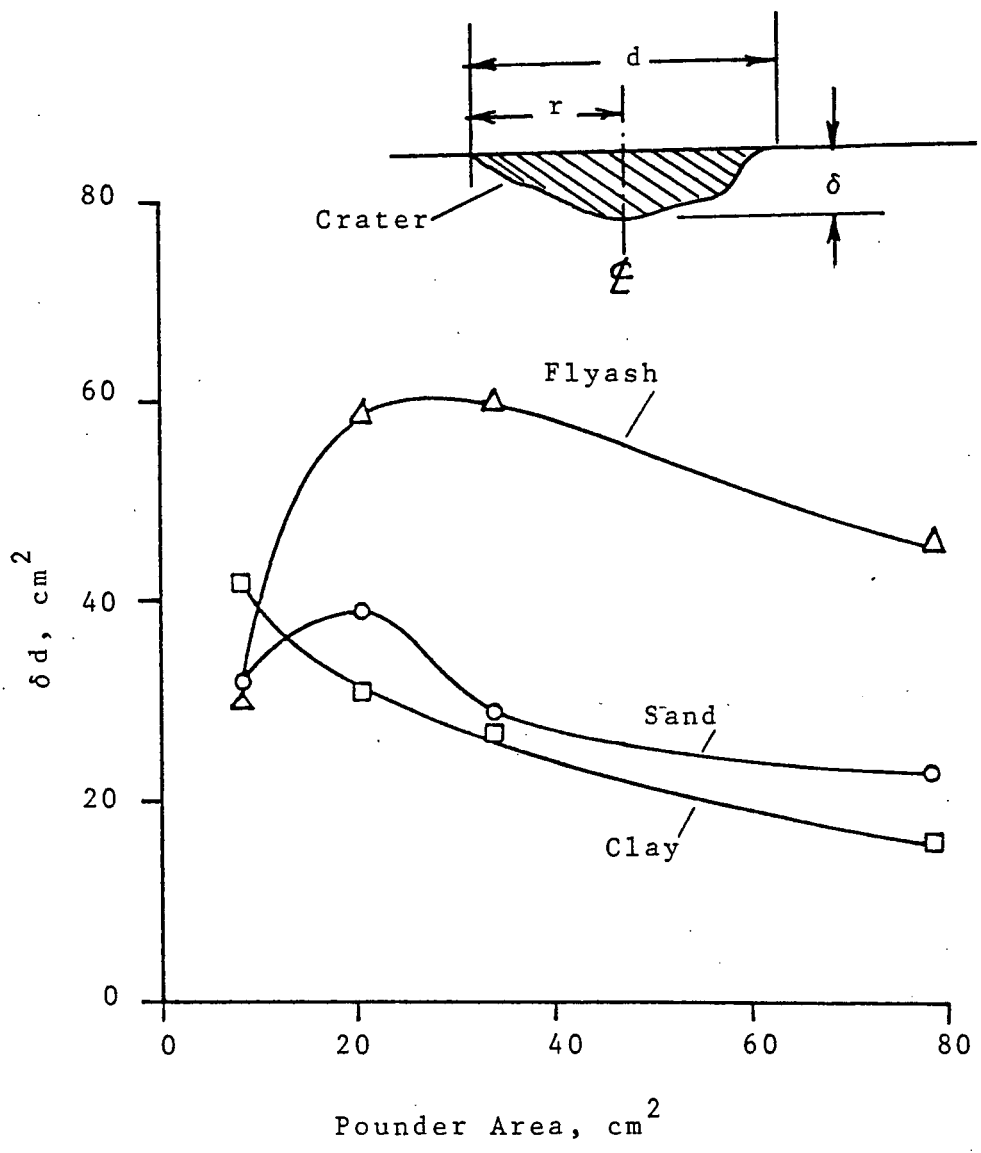


Figure 27 Crater Cross-section Area versus Pounder Area

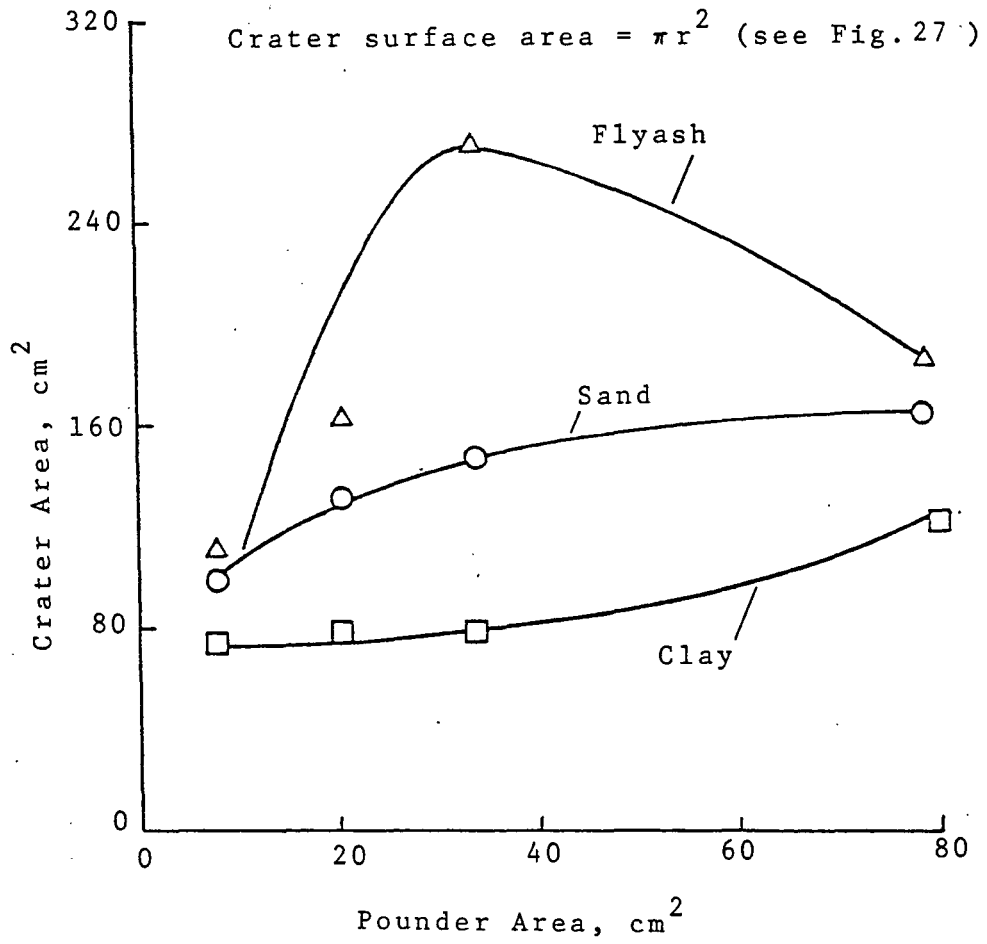


Figure 28 Crater Surface Area versus Pounder Area

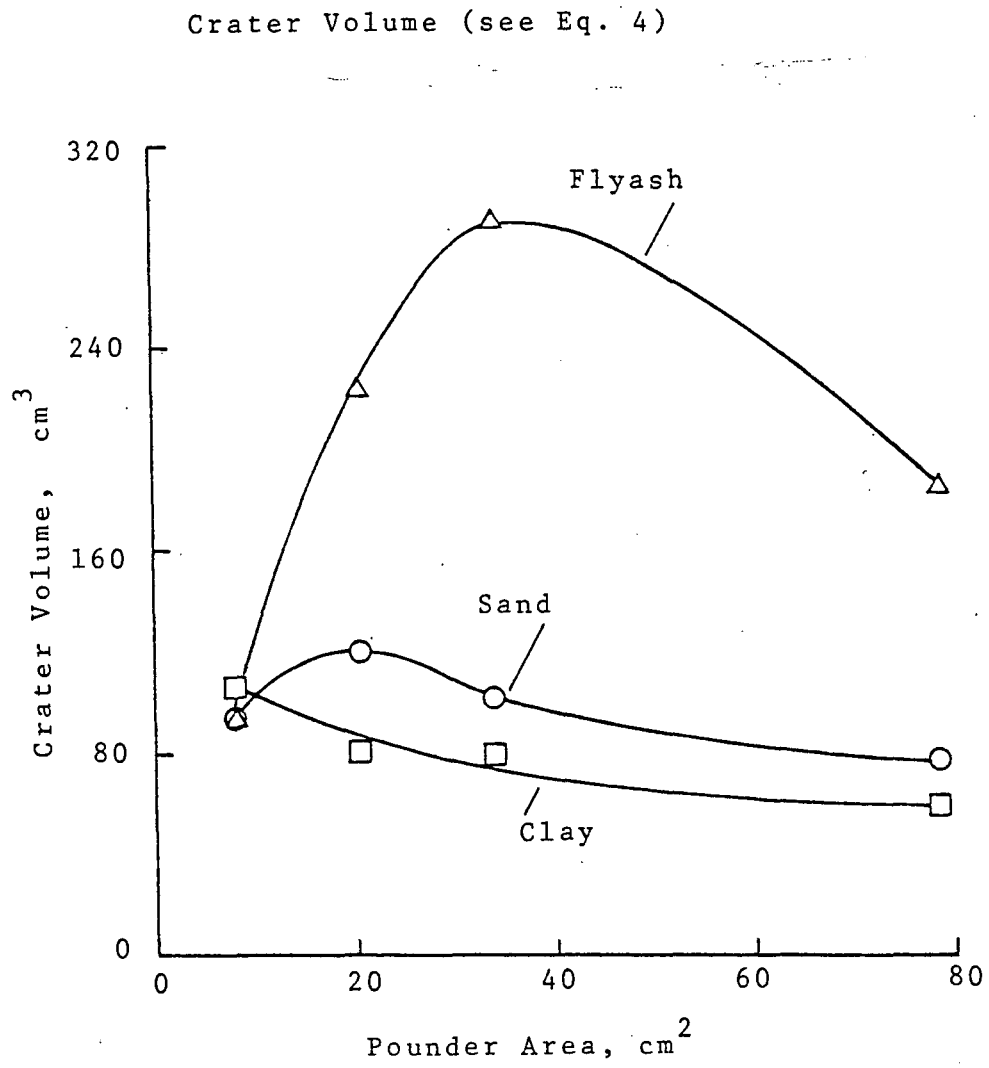


Figure 29 Crater Volume versus Pounder Area

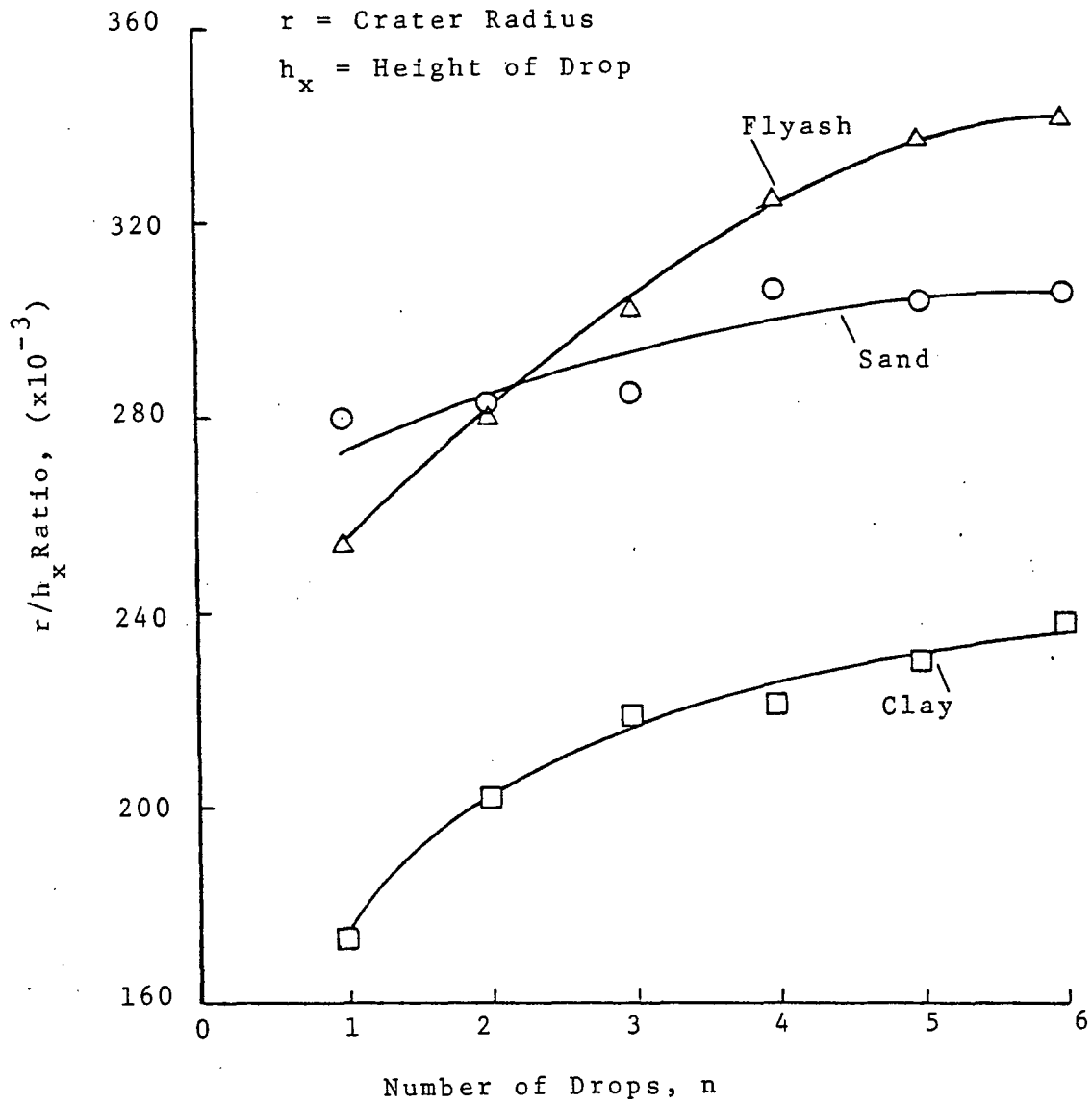


Figure 30 Crater Radius-Height of Drop Ratio versus Number of Drops

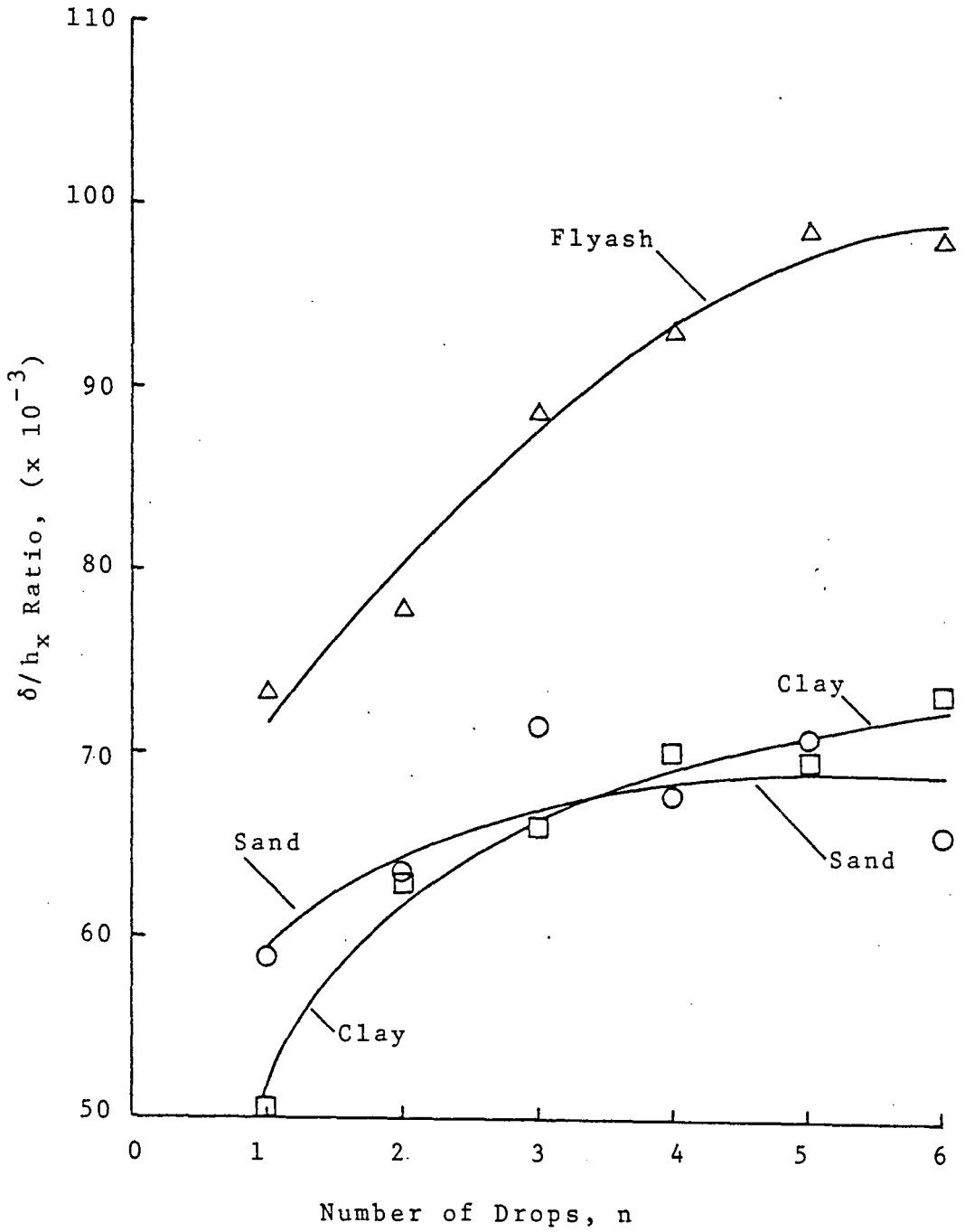


Figure 31 Crater Depth-Height of Drop Ratio versus Number of Drops

of drops is presented in Fig. 30. The ratio is higher for flyash and sand than it is for clay. It is indicated that the increase in the ratio for both flyash and clay with the number of drops is greater than sand because of side-slip phenomena as previously discussed. In both Figs. 30 and 31 the rate of increase of the ratio decreases with the number of drops. Also, in comparing Figs. 30 and 31 a similarity can be found in the shape of the curves for flyash and clay. In both Figures the slope of the flyash ratio is approximately constant up to about 4 drops when it decreases. The slope of the clay ratio shows the opposite behavior decreasing for small number of drops to an approximately constant value.

The deformation-height of drop ratio versus number of drops, n , indicates that the flyash is more greatly affected by the number of drops than sand and clay. The d/D ratio is kept constant at 0.110 for Figs. 30 and 31, where d = diameter of poulder and D is the diameter of the metal drum (see Fig. 5). Various d/D conditions have been tested; however, $d/D = 0.110$ yields the maximum r/h_x and δ/h_x ratios.

5. SUMMARY AND CONCLUSIONS

1. In all cases, for a thin layer deposit the ground response is higher. For the smaller poulder area, the effects on ground response with depth are greater in comparison with larger poulder areas. The poulder size has significant effect on ground response. However, for the thicker layer, the poulder size has little effect.
2. The higher the densification energy, the greater the ground response for all poulder sizes. However, for smaller poulder areas the ground response

is more sensitive to densification energy than larger poulder areas.

3. For the smaller poulder area, the crater area is small and the crater area increases as the poulder area increases. However, when the poulder area reaches a certain size, the crater creates the side-slip phenomena after the poulder is removed.
4. For the sand, the side-slip phenomena has greater effect in comparison with clay and flyash. In all cases, the crater area or volume of the flyash is greater than the sand and clay deposits.
5. For the sand, it is shown that heave occurs at the edge of the crater. No heave is recorded for both clay and flyash fills.
6. In all cases, increasing the number of drops increases the deformation-height of drop ratio. Clay, sand and flyash yield the same trends; however, for flyash the effects are more pronounced than for the clay and sand deposits.
7. In all cases, increasing the number of drops increases the radius of crater-height of drop ratio. However, the rate of increase for the flyash is more significant than the clay and sand deposits. A qualitative summary of Figs. 27 to 31 is presented in Table 1.
8. A further analysis will be presented in a separate report.

ACKNOWLEDGEMENT

This work was conducted under the sponsorship of Construction Materials Technology, Inc., International. Sincere thanks to Mr. Russell Longenbach for assistance in the testing program and Mr. Jeffrey C. Evans for reviewing the manuscript.

TABLE 1 QUALITATIVE SUMMARY OF FIGURES 27 TO 31

Fill Materials				
CLAY	Low	Low	Fig. 27	$\frac{\text{Crater Cross-Section Area}}{\text{Pounder Area}}$
SAND	Low	Low		
FLYASH	High	High		
CLAY	Low	Low	Fig. 28	$\frac{\text{Crater Area}}{\text{Pounder Area}}$
SAND	Medium	Medium		
FLYASH	High	High		
CLAY	Low	Low	Fig. 29	$\frac{\text{Crater Volume}}{\text{Pounder Area}}$
SAND	Low	Low		
FLYASH	High	High		
CLAY	Low	Low	Fig. 30	$\frac{\text{Crater Depth}}{\text{Height of Drop}} ; (\delta/h_x)$
SAND	Low	Low		Rate of Increase of δ/h_x with Number of Drops (n)
FLYASH	High	High		
CLAY	Low	Low	Fig. 31	$\frac{\text{Crater Radius}}{\text{Height of Drop}} ; (r/h_x)$
SAND	High	High		Rate of Increase of r/h_x with Number of Drops (n)
FLYASH	High	High		

REFERENCES

- ASCE (1978), Soil Improvement-History, Capabilities and Outlook, N.Y., 182p.
- DeBeer, E. and Wambeke, A. V. (1973), Consolidation Dynamique par Pilonnage Intensif, Aire d'Essai d'Embourg. Annales des Travaux Publics de Belgique, No. 5, October, p. 295-318.
- Hayward Baker Co. (1981), Dynamic Deep Compaction, Ground Modification Report 1223, 6p.
- Leonards, G. A., Cutter, W. A. and Holtz, R. D. (1980a), Dynamic Compaction of Granular Soils, Journal of the Geotechnical Engineering Division, Vol. 106, No. GT1, Proc. ASCE, p. 17-34.
- Leonards, G. A., Cutter, W. A. and Holtz, R. D. (1980b), Dynamic Compaction of Granular Soils, Transportation Research Record 749, p. 10-13.
- Lukas, R. G. (1980), Densification of Loose Deposits by Pounding, Journal of the Geotechnical Engineering Division, Vol. 106, No. GT4, Proc. ASCE, p. 435-446.
- Menard, L. and Broise, Y. (1975), Theoretical and Practical Aspects of Dynamic Consolidation, Geotechnique, Vol. 15, No. 1, March, p. 3-18.
- Menard Group (1978), Dynamic Consolidation, France, 24p.
- Qian, Z., Li, G. W. and Wang, W. K. (1980), Dynamic Consolidation Method for Strengthening Soft Foundation, Chinese Journal of Geotechnical Engineering, Vol. 2, No. 1, p. 27-42, (in Chinese with English summary).
- Ramaswamy, S. D., Lee, S. L. and Daulah, I. U. (1981), Dynamic Consolidation, Dramatic Way to Strengthen Soil, Civil Engineering, ASCE, April, p. 70-73.
- West, J. M. and Slocombe, B. E. (1973), Dynamic Consolidation as an Alternative Foundation, Ground Engineering, Vol. 6, No. 6, p.52-54.

Other GROUND IMPROVEMENT AND MODIFICATION Publications

Lehigh University

1. Discussion of LANDSLIDE AND FOUNDATION DESIGN, by H. Y. Fang, Proc., Intern. Conference on Planning and Design of Tall Buildings, ASCE-IABSE, Vol., 1, 1972, p. 171-172.
2. Discussion of FOUNDATION DESIGN IN MINING SUBSIDENCE AREAS, by H. Y. Fang, Proc., Regional Conference on the Planning and Design of Tall Buildings, Warsaw, Poland, Vol. 1, 1973, p. 230-231.
3. Discussion of H-BEARING PILES IN LIMESTONE AND CLAY SHALES, by H. Y. Fang, and T. D. Dismuke, Journal of the Geotechnical Engineering, Proc., ASCE, Vol. 101, No. GT6, June, 1975, p. 594-596.
4. BASIC CONSIDERATIONS OF DESIGN, CONSTRUCTION AND MAINTENANCE OF TALL BUILDING FOUNDATIONS, by H. Y. Fang, Proc., Pan-Pacific Conference on Tall Buildings, Honolulu, January, 1975, p. 186-198.
5. Discussion of LOW-COST SOIL STABILIZATION, by H. Y. Fang, Proc., 5th Pan-American Soil Mechanics and Foundation Engineering, Buenos Aires, Argentina, Nov., 1975, published in Vol. 5, 1979, p. 565-567.
6. H-PILES DRIVEN INTO DOLOMITE AND LIMESTONE FOR THE READING, PENNSYLVANIA PARKING AUTHORITY, by H. Y. Fang, and T. D. Dismuke, Associated Pile and Fitting Corporation Bulletin HPP752, 1975, 8p.
7. CORROSION PREVENTION IN GEOSTRUCTURE BY USING POLYMER-CONCRETE SYSTEMS, by H. Y. Fang and H. C. Mehta, Analysis and Design of Building Foundations, Envo Publishing Co., Inc., 1976, p. 611-635.
8. PILE FOUNDATIONS IN PINNACLED LIMESTONE REGION, by H. Y. Fang, T. D. Dismuke and H. P. Lim, Analysis and Design of Building Foundations, Envo Publishing Co., Inc., 1976, p. 771-798.
9. LANDSLIDE PROBLEMS IN TROPICAL-URBAN ENVIRONMENTS AND A CASE STUDY, by H. Y. Fang and H. K. Cheng, Analysis and Design of Building Foundations, Envo Publishing Co., Inc., 1976, p. 835-847.
10. Discussion of CURING AND TENSILE STRENGTH CHARACTERISTICS OF AGGREGATE-LIME-POZZOLAN, by H. Y. Fang, Transportation Research Record No. 560, 1976, p. 29-30.
11. STRESS-STRAIN CHARACTERISTICS OF COMPACTED WASTE DISPOSAL MATERIALS, by H. Y. Fang, R. G. Slutter and G. A. Stuebben, Proc., New Horizons in Construction Materials, Vol. 1, 1976, p. 127-138.

Other. GROUND IMPROVEMENT AND MODIFICATION Publications

Lehigh University

12. LOAD BEARING CAPACITY OF COMPACTED WASTE DISPOSAL MATERIALS, by H. Y. Fang, R. G. Slutter and R. M. Koerner, Specialty Session on Geotechnical Engineering and Environmental Control, 9th Intern. Conference on Soil Mechanics and Foundation Engineering, Tokyo, Japan, July, 1977, p. 265-278.
13. PLANNING AND DESIGN OF TALL BUILDING FOUNDATIONS ON SLOPING HILLSIDES, by H. Y. Fang and H. K. Cheng, Proc., 2nd Hong Kong Conference on Tall Buildings, September, 1976, p. 279-297.
14. LANDSLIDE PROBLEMS IN TROPICAL-EARTHQUAKE REGION, by H. Y. Fang, Proc., Meeting on Landslide-Earthquake Engineering, U.S.-CHINA Cooperative Research Program, National Science Foundation, Taipei, Taiwan, August, 1977, p. 233-252.
15. REINFORCED EARTH WITH SULPHUR-SAND TREATED BAMBOO EARTH-MAT, by H. Y. Fang, Proc., Symposium on Soil Reinforcing and Stabilising Techniques in Engineering Practice, Sydney, Australia, October, 1978, p. 191-200.
16. USE OF SULPHUR-TREATED BAMBOO FOR LOW-VOLUME ROAD CONSTRUCTION, by H. Y. Fang, Transportation Research Record 702, August, 1979, p. 147-154.
17. ENGINEERING, CONSTRUCTION AND MAINTENANCE PROBLEMS IN LIMESTONE REGIONS, edited by T. D. Dismuke and H. Y. Fang, Symposium Proc., ASCE Lehigh Valley Section, August 3-4, 1976, published in January, 1979, 207p.
18. USING COMPOSITE-BAMBOO PILES FOR CONTROLLING LANDSLIDES IN EARTHQUAKE REGIONS, by H. Y. Fang, Proc. Intern. Conference on Engineering for Protection from Natural Disasters, Bangkok, Thailand, 1980, p. 23-34.
19. BAMBOO-LIME COMPOSITE PILE-A NEW LOW-COST REINFORCED EARTH SYSTEM, by H. Y. Fang, T. R. Moore and M. F. Rovi, Proc., 3rd. Conference of the Road Engineering Association of Asia and Australasia, Taipei, Taiwan, April 20-24, 1981, p. 413-427.
20. LOW-COST CONSTRUCTION MATERIALS AND FOUNDATION STRUCTURES, by H. Y. Fang, Proc., 2nd Australian Conference on Engineering Materials, Sydney, July, 6-8, 1981, p. 39-48.
21. INFLUENCE OF PORE FLUID ON CLAY BEHAVIOR, by J. C. Evans, R. C. Chaney and H. Y. Fang, Fritz Engineering Laboratory Report No. 384.14, Lehigh University, December, 1981, 67p.

Other GROUND IMPROVEMENT AND MODIFICATION Publications

Lehigh University

22. GEOTECHNICAL ASPECTS OF THE DESIGN AND CONSTRUCTION OF WASTE CONTAINMENT SYSTEMS, by J. C. Evans and H. Y. Fang, Proc. 3rd. National Conf. on Management of Uncontrolled Hazardous Waste Sites, Washington, D. C., p. 175-182. 1982.
23. DYNAMIC PROPERTIES OF FLYASH, by H. Y. Fang, R. C. Chaney and J. A. Stefanik, Proc. International Conf. on Soil Dynamics and Earthquake Engineering, University of Southampton, U.K., 1982, p. 103-111.
24. REVIEW OF CAVITY EXPANSION MODELS IN SOIL AND ITS APPLICATIONS, by N. S. Pandit, R. C. Chaney and H. Y. Fang, Fritz Engineering Laboratory Report No. 462.10, March, 1983, Lehigh University, 27p.
25. LABORATORY STUDY OF DYNAMIC DENSIFICATION OF FLYASH, by H. Y. Fang, G. W. Ellis and R. C. Chaney, Fritz Engineering Laboratory Report No. 462.10, Lehigh University, March, 1983, 16p.
26. DYNAMIC RESPONSE TO FLYASH, by R. C. Chaney, H. Y. Fang and G. W. Ellis, Proc. ASCE Specialty Conf. on Engineering Mechanics Div., Purdue University, May, 1983.
27. LABORATORY STUDY OF GROUND RESPONSE TO DYNAMIC DENSIFICATION, by H. Y. Fang and G. W. Ellis, Fritz Engineering Laboratory Report No. 462.6, Lehigh University, March, 1983, 44p.
28. MECHANISM OF SOIL CRACKING, by H. Y. Fang, R. C. Chaney, R. A. Failmezger and J. C. Evans, Proc. 20th Annual Meeting of the Society of Engineering Science, University of Delaware, August, 1983.